

**SYNTHESIS AND CHARACTERISATION OF SCHIFF BASE
LIQUID CRYSTALS POSSESSING DIALKYLAMINO TERMINAL
UNIT**

BONG SZE HAO

BACHELOR OF SCIENCE (HONS.) CHEMISTRY

FACULTY OF SCIENCE

UNIVERSITI TUNKU ABDUL RAHMAN

MAY 2011

BONG SZE HAO

B. Sc. (Hons.) Chemistry

2011

**SYNTHESIS AND CHARACTERISATION OF SCHIFF BASE LIQUID
CRYSTALS POSSESSING DIALKYLAMINO TERMINAL UNIT**

BY

BONG SZE HAO

A project report submitted to the Department of Chemical Science,
Faculty of Science,
Universiti Tunku Abdul Rahman,
in partial fulfillment of the requirements for the degree of
Bachelor of Science (Hons) Chemistry
May 2011

ABSTRACT

A series of Schiff's base ester, 4-((4-(dimethylamino)benzylidene)amino)phenyl-4-(alkanoyloxy)benzoates, **nDMABAPB**, where n denotes the number of carbons in the straightalkyl chain (n = 10, 12, 14, 16 and 18), were successfully synthesized, characterized and the mesomorphic properties were investigated.

The products were synthesized in two major steps. The first step involved condensation reaction between 4-aminophenol and 4-(dimethylamino)benzaldehyde which produced the imine linkage of the two aromatic rings. The intermediate compound formed was (E)-4-((4-(dimethylamino)benzylidene)amino)phenol, **DMABAP**. The second step of the synthesis involved the Steglich esterification between the **nDMABAP** and the 4-alkyloxybenzoic acids, **nABA**.

The structures of the synthesized compounds were confirmed by infrared (IR), ¹H and ¹³C Nuclear Magnetic Resonance (NMR), as well as Electron-Ionisation Mass (EI-MS) spectroscopic techniques. Differential Scanning Calorimetry (DSC) and Polarising Optical Microscopy (POM) were used to study the thermal and mesomorphic properties of the compounds. All the compounds **nDMABAPB** where n = 10, 12, 14, and 16 exhibited a thread-like texture nematic phase on cooling from the isotropic liquid only. However, for **18DMABAPB**, it exhibited both smectic C and nematic phase upon cooling.

ABSTRAK

Siri ester berpangkalan Schiff, (E)-4-((4-(dimetilamino)benziliden)amino)fenil-4-(alkanoyloxy)benzoat, **nDMABAPB**, di mana n menunjukkan jumlah karbon pada rantai alkil lurus (n = 10, 12, 14, 16 dan 18), berjaya disintesis, ditandai dan sifat mesomorphic diselidiki.

Produk disintesis dalam dua langkah utama, reaksi yang pertama adalah kondensasi diantara 4-aminofenol dan 4-(dimetilamino)benzaldehid untuk menghasilkan hubungan imina dari dua cincin aromatik. Sebatian pertengahan yang terbentuk adalah (E)-4-((4-(dimetilamino)benziliden)amino)fenol, DMABAP. Langkah kedua melibatkan sintesis pengesteran Steglich antara **nDMABAP** dan asid benzoat, **nABA**.

Struktur sebatian yang disintesis disahkan dengan inframerah (IR), ^1H dan ^{13}C Resonans Magnet Nukleus (NMR), serta elektron-pengionan jisim (EI-MS) teknik spektroskopi. Kalorimetri Perbezaan Pengimbasan (DSC) dan Pengkutuban Mikroskop Optik (POM) digunakan untuk mempelajari sifat terma dan mesomorphic daripada sebatian yang disintesis. Semua **nDMABAPB** sebatian mana n = 10, 12, 14, dan 16 menunjukkan fasa tekstur benang-seperti nematic pendingin dari cairan isotropik saja. Namun, untuk **18DMABAPB**, itu dipamerkan baik C smectic dan fasa nematic pada saat pendinginan.

ACKNOWLEDGEMENTS

First of all, I would like to express my gratitude towards the Faculty of Science of Universiti Tunku Abdul Rahman for giving me the opportunity to carry out a lab scale research on liquid crystals. This however indeed has given me a chance in learning more on carrying my lab skills and analysis abilities during the time carrying my research project. I believe through this final year project will equip myself and prepare me towards the actual job situation upon graduation.

Besides that, I would also like to express my deepest gratitude towards my project supervisor, Assistant Professor Dr. Ha Sie Tiong for his advice, patience, and wealth of knowledge from synthesis and liquid crystals to trivial facts. Apart of this, I would also like to express my appreciation Professor Dr. Yeap Guan Yeow from Universiti Sains Malaysia for kindly allowing us to visit and carry out various analyses using the university's equipment. I would like to express my gratitude as well to my seniors, Mr. Foo Kok Leei and Mr. Lee Teck Leong for their help throughout this project.

Last but not least, I would also express my deepest gratitude to my family members and friends which supported me throughout my project. Without their support, I think I might not be able to complete my thesis as well.

APPROVAL SHEET

I certify that, this project report entitled **“SYNTHESIS AND CHARACTERISATION OF MESOGENIC SCHIFF BASE ESTER,4-((4-DIMETHYLAMINO)BENZYLIDENE)AMINO)PHENYL-4-(ALKANOYLOXY)BENZOATE”** was prepared by BONG SZE HAO and submitted in partial fulfilment of the requirements for the degree of Bachelor of Science(Hons.) in Chemistry at Universiti Tunku Abdul Rahman.

APPROVED by

Supervisor

Date: _____

(Assistant Professor Dr. Ha SieTiong)

FACULTY OF SCIENCE
UNIVERSITI TUNKU ABDUL RAHMAN

Date: _____

PERMISSION SHEET

It is hereby certified that BONG SZE HAO (ID No: 08ADB02984) has completed this report entitled **“SYNTHESIS AND CHARACTERISATION OF MESOGENIC SCHIFF BASE ESTER,4-((4-DIMETHYLAMINO)BENZYLIDENE)AMINO)PHENYL-4-(ALKANOYLOXY)BENZOATE”** under supervision of Assistant Professor Dr. Ha SieTiong from the Department of Chemical Science, Faculty of Science.

I hereby give permission to my supervisors to write and prepare manuscript of these research findings for publishing in any form, if I did not prepare it within six(6) months' time from this date provided that my name is included as one of the author for this article. Arrangement of the name depends on my supervisors.

DECLARATION

I hereby declare that the project report is based on my original work except for quotations and citations which have been duly acknowledged. I also declare that it has not been previously or concurrently submitted for any other degree at UTAR or other institutions.

BONG SZE HAO

Date:

TABLE OF CONTENTS		Pages
ABSTRACT		i
ABSTRAK		ii
ACKNOWLEDGEMENTS		iii
APPROVAL SHEET		iv
PERMISSION SHEET		v
DECLARATION		vi
TABLE OF CONTENTS		vii
LIST OF TABLES		x
LIST OF FIGURES		xi
LIST OF ABBREVIATION		xiv
LIST OF APPENDICES		xvii
CHAPTER		
1 INTRODUCTION		1
1.1 Introduction to Liquid Crystal		1
1.1.1 History and Development of Liquid Crystals		3
1.2 Categories of Liquid Crystals		6
1.2.1 Calamitic Liquid Crystals		8
1.2.2 Liquid Crystals Phases		11
1.3 Applications of Liquid Crystals		15
1.4 Objectives		19

2	LITERATURE REVIEW	20
2.1	Schiff Base Liquid Crystals	20
2.2	Structure-Mesomorphic Properties Relationship	22
2.2.1	Influence of Terminal Units	22
2.2.2	Influence of Core group	25
2.2.3	Influences of Chain Lengths	27
2.2.4	Influence of Lateral Substituents	30
3	MATERIALS AND METHODOLOGY	34
3.1	Chemicals	34
3.2	Instruments	35
3.3	Synthesis	37
3.3.1	Synthesis of DMABAP	38
3.3.2	Synthesis of nABA	38
3.3.3	Synthesis of nDMABAPB	39
3.3.3.1	Synthesis of 10DMABAPB	39
3.3.3.2	Synthesis of 12DMABAPB	40
3.3.3.3	Synthesis of 14DMABAPB	41
3.3.3.4	Synthesis of 16DMABAPB	41
3.3.3.5	Synthesis of 18DMABAPB	42
3.4	Characterization	42
3.4.1	Infrared Spectral Analysis	42
3.4.2	Thin Layer Chromatography	43

	¹ H and ¹³ C Nuclear Magnetic Resonance	43
	3.4.4 Mass Spectroscopy Analysis	44
	3.4.5 Differential Scanning Calorimetry	44
	3.4.6 Polarized Optical Microscopy Analysis	45
4	RESULTS AND DISCUSSION	46
	4.1 Structure Elucidation	46
	4.1.1 Thin Layer Chromatographic Analysis	46
	4.1.2 FTIR Analysis	48
	4.1.2.1 Infrared Spectral Analysis on DMABAP	48
	4.1.2.2 Infrared Spectral Analysis on nABA	51
	4.1.2.3 Infrared Spectral Analysis on nDMABAPB	53
	4.1.3 Nuclear Magnetic Resonance Analysis	58
	4.1.3.1 ¹ H NMR Spectra for 12DMABAPB	58
	4.1.3.2 ¹³ C NMR Spectra for 12DMABAPB	63
	4.1.4 Mass Spectrometry Analysis of 16DMABAPB	67
	4.2 Mechanism of Steglich Esterification	70
	4.3 Mesomorphic Properties Analysis of nDMABAPB	73
	4.3.1 DSC Thermogram Analysis of nDMABAPB	73
	4.3.2 Influence of alkyl chains	75
	4.4 Polarising Optical Microscopy Studies of nDMABAPB	79
	4.5 Structural Comparison with Related Compounds	82
5	CONCLUSION	85
	FUTURE STUDY	86
	REFERENCES	87

LIST OF TABLES

Table		page
2.1	Overall transition temperatures measured on heating for the ω -unsaturated derivatives. Cr, SmX, SmA, and I indicate crystal, smectic X, smectic A, and isotropic phases respectively	26
3.1	List of Instruments used in this Project	36
4.1	FTIR value for n-alkyloxybenzoic acid	51
4.2	FTIR data for nDMABAPB	55
4.3	FTIR value for 4AP , DMABAP and 12DMABAPB	56
4.4	¹ HNMR data and the proposed structure of 12DMABAPB	59
4.5	¹³ C NMR data and the proposed structure of 16DMABAPB	65
4.6	Mass Spectrometry data of 16DMABAPB	70
4.7	Transition temperatures of compounds nDMABAPB , where n= 10, 12, 14, 16 and 18, upon heating and cooling, obtained from DSC	76
4.8	Transition temperature (°C) for 10DMABAPB , 10DBDMAA , and CBDAAB	83

LIST OF FIGURES

Figure	page
1.1	Overlap of the properties of liquid crystals with solid and liquid 1
1.2	(a) Arrangement of molecules in a crystalline solid. (b) Arrangement of molecules in a liquid crystal. (c) Arrangement of molecules in a liquid. 2
1.3	(a) A schematic representation of a rod shaped liquid crystal. 7 (b) A schematic representation of a disc shaped liquid crystal
1.4	Classification of Liquid Crystal 8
1.5	Molecular structure of a typical liquid crystal 9
1.6	General structure of calamitic liquid crystal 11
1.7	Texture and molecular arrangement of typical nematic liquid crystal 12
1.8	(a) Texture and molecular arrangement of typical smectic A liquid crystal (b) Texture and molecular arrangement of typical smectic C liquid crystal (c) Texture and molecular arrangement of typical smectic C* liquid crystal 13
1.9	Texture and molecular arrangement of typical cholesteric liquid crystal 14
1.10	Some of the application of liquid crystals 18
2.1	Mechanism of imine formation 21
2.2	Structure of 3-hydroxy-4-[(4-X- substitutedphenyl)imino]methyl}phenyloctadecanoate 23
2.3	Structure of the series Phm, Bm, PhBm 25
2.4	4-chlorobenzylidene-4-alkanoyloxyanilines, nCIBA 27

2.5	General structures of the ionic liquid crystals with different core sizes and imidazolium group for lateral substitution	29
2.6	Structures of 2-hydroxy-4-methoxybenzylidene-4'-alkanoyloxyaniline (series A), 2-hydroxy-3-methoxybenzylidene-4'-alkanoyloxyaniline (series B) and 3-methoxy-4-alkanoyloxybenzylidene-4'-alkanoyloxyaniline (series C) upon heating (Yeapet <i>al.</i> , 2006).	30
2.7	Structure of (R)-2-Fluoro-4-[1-methyl-2-(2,2,3,3,3-pentafluoropropoxy)ethyloxycarbonyl]phenyl 4'-alkyloxybiphenyl-4-carboxylates(2F) and (R)-3-Fluoro-4-[1-methyl-2-(2,2,3,3,3-pentafluoropropoxy)ethyloxycarbonyl]phenyl 4'-alkyloxybiphenyl-4-carboxylates(3F), where (m = 8-12)	33
3.1	Reaction scheme of intermediate DMABAP and final compound, nDMABAPB	37
4.1	Sketch of TLC plates for 12DMABAPB	47
4.2	IR Spectra of 4AP , 4DMAB , and DMABAP	50
4.3	FTIR Spectrum of 12ABA	52
4.4	IR Spectrum of 12DMABAPB	54
4.5	Comparison of FTIR of 4AP , DMABAP and 12DMABAPB	57
4.6	¹ H-NMR spectrum of 12DMABAPB	62
4.7	¹³ C-NMR spectrum of 16DMABAPB	66
4.8	Mass Spectrum of 16DMABAPB	69
4.9	Reaction mechanism of DCC with imine and carboxylic acid	71
4.10	Function of DMAP	72
4.11	DSC thermogram of 18DMABAPB	73
		78

- 4.12 Graph of Transition Temperature versus Number of Carbons on Alkyl Chain
- 4.13 Optical photomicrograph of taken during cooling cycle. (a) Optical photomicrograph of compound **10DMABAPB** exhibiting thread-like textures of nematic phase (b) Optical photomicrograph of **18DMABAPB** exhibiting transition from nematic phase to (c) marble-like texture of SmC phase 80
- 4.14 Structural Comparison with related compounds reported in the literature 82

LIST OF ABBREVIATION

LC	Liquid Crystal
4AP	4-Aminophenol
DMABAP	(E)-4-((4-(dimethylamino)benzylidene)amino)phenol
nDMABAPB	(E)-4-((4-(dimethylamino)benzylidene)amino)phenyl-4-(alkanoyloxy)benzoate
¹³ C NMR	Carbon-13 Nuclear Magnetic Resonance
¹ H NMR	Proton Nuclear Magnetic Resonance
DSC	Differential Scanning Calorimetry
MS	Mass Spectroscopy
POM	Polarised Optical Microscopy
FTIR	Fourier Transform Infrared
TLC	Thin Layer Chromatography
CDCl ₃	Deuterated Chloroform
DCC	N,N'-Dicyclohexylcarbodiimide
DCM	Dichloromethane
DMAP	4-Dimethylaminopyridine
DMF	Dimethylformamide

THF	Tetrahydrofuran
mmol	milimol
ppm	parts per million
nDMABAPB	4-((4-(dimethylamino)benzylidene)amino)phenyl-4-(alkanoyloxy)benzoate
10DMABAPB	4-((4-(dimethylamino)benzylidene)amino)phenyl-4-(decyloxy)benzoate
12DMABAPB	4-((4-(dimethylamino)benzylidene)amino)phenyl-4-(dodecyloxy)benzoate
14DMABAPB	4-((4-(dimethylamino)benzylidene)amino)phenyl-4-(tetradecyloxy)benzoate
16DMABAPB	4-((4-(dimethylamino)benzylidene)amino)phenyl-4-(hexadecyloxy)benzoate
18DMABAPB	4-((4-(dimethylamino)benzylidene)amino)phenyl-4-(octadecyloxy)benzoate
nABA	4-Alkyloxybenzoic acid
10ABA	4-Decyloxybenzoic acid
12ABA	4-Dodecyloxybenzoic acid
14ABA	4-Tetradecyloxybenzoic acid
16ABA	4-Hexadecyloxybenzoic acid
18ABA	4-Octadecyloxybenzoic acid
N	Nematic
Sm	Smectic
I	Isotropic
Cr	Crystal

LIST OF APPENDICES

	Page	
A1	FTIR Spectrum of 10ABA	91
A2	FTIR Spectrum of 14ABA	92
A3	FTIR Spectrum of 16ABA	93
A4	FTIR Spectrum of 18ABA	94
A5	FTIR Spectrum of 10DMABAPB	95
A6	FTIR Spectrum of 14DMABAPB	96
A7	FTIR Spectrum of 16DMABAPB	97
A8	FTIR Spectrum of 18DMABAPB	98
B1	DSC Thermogram for 10DMABAPB	99
B2	DSC Thermogram for 12DMABAPB	100
B3	DSC Thermogram for 14DMABAPB	101
B4	DSC Thermogram for 16DMABAPB	102

CHAPTER 1

INTRODUCTION

1.1 Introduction to Liquid Crystals

Liquid crystals are unique compounds discovered ever. It is an extension to the studies on intermediates phases between the two common condensed matter phases which are solid crystalline and liquid phases (Khoo, 2007). Liquid crystals exhibit the intermediate phases where it can diffuse freely like liquids but somehow it also retains some physics properties characteristic of solid crystalline (Collings *et al.*, 1998).

Liquid crystals are substances that exhibit a phase of matter that has properties between those of a conventional liquid, and those of a solid crystal, as shown in Figure 1.1.

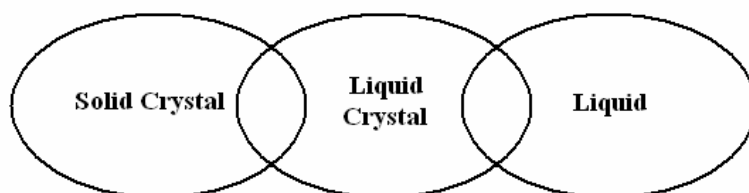


Figure 1.1: Overlap of the properties of liquid crystals with conventional solid crystals and liquid

In a solid state, molecules are arranged very close together and cannot move around which shown in the Figure 1.2 (a). It is in a regular structure, which arranged in a well ordered pattern. Crystalline solids have molecules that are arranged in fixed geometric patterns or lattices with repeating unit cells extending in all three spatial dimensions. As shown in Figure 1.2 (c), the molecules in a liquid are close together but do not have fixed positions and can move around freely. In contrast, the molecules in a liquid crystal have an arrangement of that in between a solid and a liquid as shown in the Figure 1.2(b). They can be considered to be crystals which have lost some or all of their positional order, while maintaining full orientational order or as a liquid whose component particles, atoms or molecules, tend to arrange themselves with a degree of order far exceeding that found in ordinary liquids and approaching that of solid crystals (Singh, 2002).

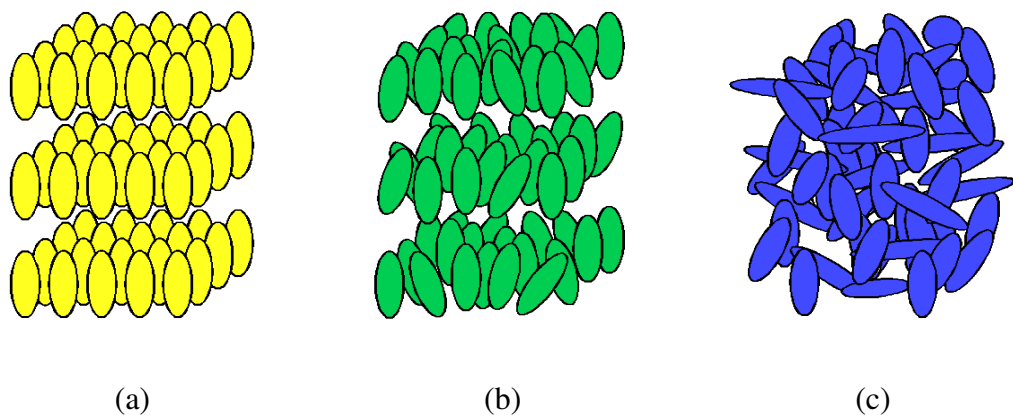


Figure 1.2: (a) Arrangement of molecules in a crystalline solid
(b) Arrangement of molecules in a liquid crystal
(c) Arrangement of molecules in a liquid

In a liquid crystal, as in an ordinary liquid, the positions of the molecules are not as orderly as compared to those in the solid. Liquid crystals generally have molecules which are long and thin in shape. Thus, even if the molecular positions are random, their orientation can be aligned in a regular pattern giving rise to the ordered structure of a liquid crystal (Singh, 2002). Consequently, they are observed to physically flow like liquids, but they have many of the optical properties of solid crystals and material properties such as permittivity, refractive index, elasticity and viscosity which are anisotropic (*i.e.*, their magnitude will differ from one direction to another). And since the order is not as firmly fixed as that of a solid crystal, they can be easily modified with corresponding changes in the optical properties. Liquid crystals can be found as the slimy substance at the bottom of a soap dish and as the material in a laptop screen (Collings *et al.*, 1998).

1.1.1 History and Development of Liquid Crystals

Between 1850 and 1888, researchers in different fields such as chemistry, biology, medicine and physics found that several materials behaved strangely at temperatures near their melting points. It was observed that the optical properties of these materials changed discontinuously with increasing temperatures. W. Heintz, for example, reported in 1850 that stearin melted from a solid to a cloudy liquid at 52 °C, changed at 58 °C to an opaque and at 62.5 °C to a clear liquid. Others reported observing blue colour when compounds synthesized from

cholesterol were cooled. Biologists observed anisotropic optical behaviour in "liquid" biological materials, behaviour usually expected only in the crystal phase (Ici.kent, 2010).

An important invention of the time was the heating stage microscope by Otto Lehmann, a physicist from Karlsruhe, Germany. This microscope allowed control of the temperature of the sample. In a later version, with polarisers added, it became the standard equipment in every liquid crystal research laboratory (Ici.kent, 2010).

In 1888, the Austrian chemist Friedrich Reinitzer, working in the Institute of Plant Physiology at the University of Prague, discovered a strange phenomenon. Reinitzer was conducting experiments on a cholesterol based substance trying to figure out the correct formula and molecular weight of cholesterol. When he tried to precisely determine the melting point, which is an important indicator of the purity of a substance, he was struck by the fact that this substance seemed to have two melting points. At 145.5 °C the solid crystal melted into a cloudy liquid which existed until 178.5 °C where the cloudiness suddenly disappeared, giving way to a clear transparent liquid. At first Reinitzer thought that this might be a sign of impurities in the material, but further purification did not bring any changes to this behaviour (Khoo, 2007).

Puzzled by his discovery, Reinitzer turned for help to the German physicist Otto Lehmann, who was an expert in crystal optics. Lehmann became convinced that the cloudy liquid had a unique kind of order. In contrast, the transparent liquid at higher temperature had the characteristic disordered state of all common liquids. Eventually he realized that the cloudy liquid was a new state of matter and coined the name "liquid crystal," illustrating that it was something between a liquid and a solid, sharing important properties of both. In a normal liquid the properties are isotropic, i.e. the same in all directions. In a liquid crystal they are not; they strongly depend on direction even if the substance itself is fluid (Khoo, 2007).

This new idea was challenged by the scientific community, and some scientists claimed that the newly-discovered state probably was just a mixture of solid and liquid components. In 1922 in Paris, France, Georges Freidel suggested the classification scheme which is used today with different phases of liquid crystals called nematic, smectic and cholesteric (Ici.kent, 2010).

In the 1960s, a French theoretical physicist, Pierre-Gilles de Gennes, who had been working with magnetism and superconductivity, turned his interest to liquid crystals and soon found fascinating analogies between liquid crystals and superconductors as well as magnetic materials. His work was rewarded with the Nobel Prize in Physics 1991. The modern development of liquid crystal science

has since been deeply influenced by the work of Pierre-Gilles de Gennes (Nobelprize, 2010).

Today, thanks to Reinitzer, Lehmann and their followers, we know that literally thousands of substances have a diversity of other states. Some of them have been found very usable in several technical innovations, among which liquid crystal screens and liquid crystal thermometers may be the best known.

1.2 Categories of Liquid Crystals

Compounds consist such unusual phases are also known as mesogens and their various phases in which they can exist are termed as mesophases (Khoo, 2007). Liquid crystals are grouped into a few general groups which are well-known and widely studied such as thermotropics, lyotropics, and metallotropic phases (Khoo, 2007). There are lots of different types of molecules form liquid crystals phases at various temperature and pressure. At atmospheric pressure, if temperature is the major physical variable in determines a liquid crystal's phase, that particular types of liquid crystals are termed as thermotropic liquid crystals. Meanwhile, there are other types of liquid crystalline materials which formed from anisotropic objects immersed in a solvent. The phases of these materials are mainly determined by the composition of the mixture. These types of liquid

crystals are termed as lyotropic liquid crystals (Fisch, 2006). Lyotropic liquid crystals commonly exhibit in disk shaped or rod shaped. Figure 1.3 below shown typical rod shaped or disk shaped liquid crystal:

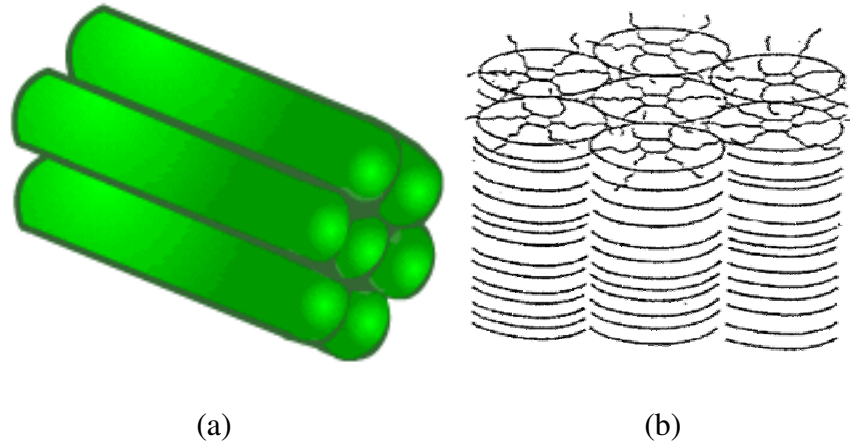


Figure 1.3: (a) A schematic representation of a rod shaped liquid crystal
(b) A schematic representation of a disc shaped liquid crystal

Here, we will focus more on the thermotropic liquid crystals because it is the most widely studied and used types of liquid crystals. There are two classifications of thermotropic liquid crystals based on their molecular mass. Low molecular mass thermotropic liquid crystals are subdivided into three which are calamitic, discotic and sematic. Calamitic refers to rod-shaped liquid crystals, whereas discotic and sematic refer to disc-shaped and lath-shaped. The general classification of liquid crystals is shown in Figure 1.4.

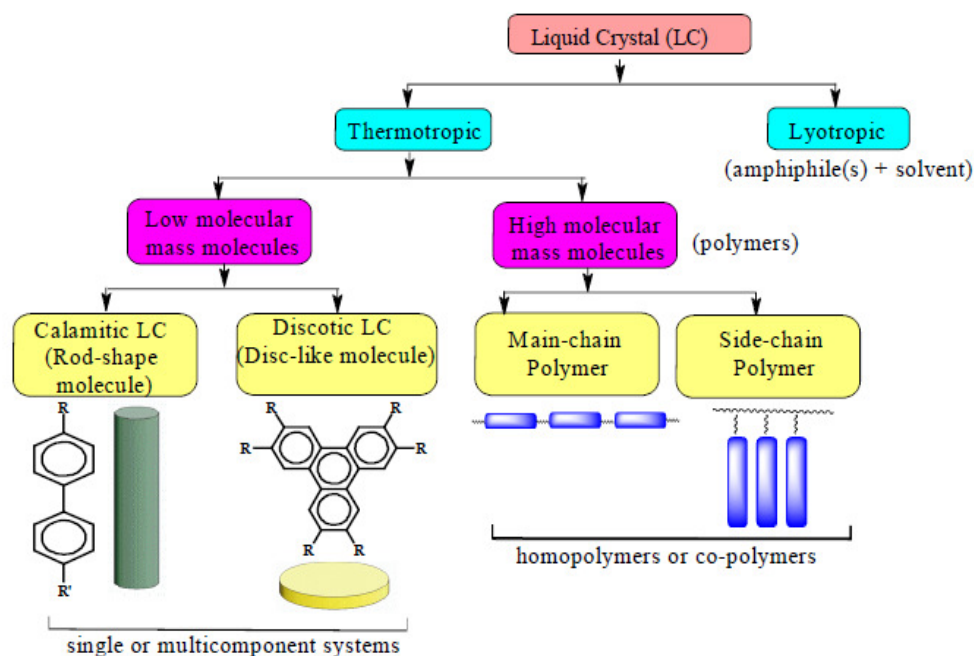


Figure 1.4: Classification of Liquid Crystal (Gray *et al.*, 1983)

1.2.1 Calamitic Liquid Crystals

A compound must possess a certain requirement in order to exhibit liquid crystals properties. Figure 1.5 provides the basic structure of the most commonly occurring liquid crystals. A typical example of aromatic compounds contained benzene rings which may also referred as benzene derivatives.

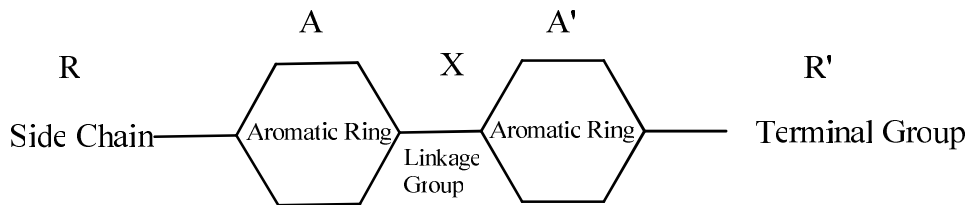


Figure 1.5: Molecular structure of a typical liquid crystal

Examples of side-chain and terminal groups are alkyl (C_nH_{2n+1}), alkoxy ($C_nH_{2n+1}O$), and others such as acyloxy, alkylcarbonate, alkoxy-carbonyl, nitro, and cyano groups. The Xs of the linkage groups are simple bonds or groups such as stilbene ($-CH=CH-$), ester ($-COO-$), Schiff base ($-CH=N-$), azoxy ($-N=N-$), acetylene ($-C\equiv C-$), and diacetylene ($-C\equiv C-C\equiv C-$). The names of liquid crystals are often termed after the linkage group like Schiff-base liquid crystal. There are few types of aromatic available. These include saturated cyclohexane, unsaturated phenyl, biphenyl, terphenyl in various combinations. The majority of liquid crystals are benzene derivatives which have mentioned previously (Khoo, 2007).

Heterocyclic liquid crystals are very similar in structure with benzene derivatives, with one or more of the benzene rings replaced by a pyridine, pyrimidine, or other similar groups. Cholesterol derivatives are the most common form of chemical compounds that exhibit the cholesteric which also termed as chiral nematic phase of liquid crystals. Organometallic compounds are special in

that they contain metallic atoms and possess interesting dynamical and magneto-optical properties (Khoo, 2007).

After years of research that has carried on liquid crystals, researchers have come out general requirements on the structures of liquid crystals. Firstly, the molecule of a compound which has liquid crystal properties must be in elongated shape where its length should be more than its width. Such elongated molecules must possess stronger attractive forces. These molecules must also have fewer tendencies to collide with each other as they tend to point to the same direction. This helps to stabilise the whole structure of the compound.

Besides that, the molecules must also have certain amount of rigidity in its core region. Then, it added its advantages if the ends of the molecules are flexible. The flexibility allows one molecule to place itself easily between others molecules when move around. Both flexibility and rigidity must be in balance in order to exhibit liquid crystal properties (Fisch, 2006). The Figure 1.6 shows the general structure of calamitic liquid crystal.

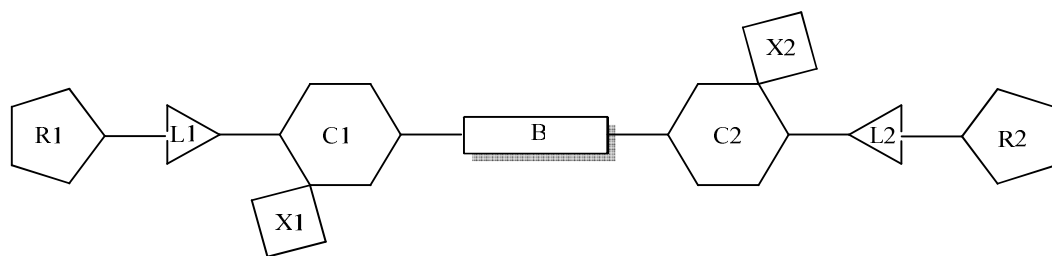


Figure 1.6: General structure of Calamitic liquid crystal

Where,

C = core groups (aromatic ring)

R = terminal group (alkyl chain)

X = lateral substituent on core group (hydroxyl, halogen)

B & L = bridging group (ester, imine, etc.)

1.2.2 Liquid Crystals Phases

i) Nematic Phase:

The nematic phase is the least ordered liquid crystal phase, with molecules only possessing orientational order, but no positional order. Thus it is usually the least viscous mesophases. The preferred direction, *i.e.* the direction, where the long axis of the molecule is most likely to point, is called the director, usually **n**. Figure 1.7 shows this phase (Wikipedia, 2010).

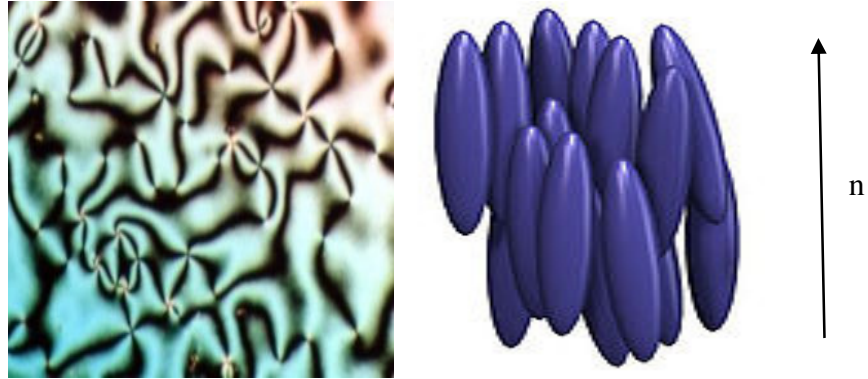


Figure 1.7: Texture and molecular arrangement of typical nematic liquid crystal

ii) Smectic Phase:

Smectic phases show orientational order, and also some positional order. The molecules are preferably pointing in one direction, just like in the nematic phase. Additionally, the molecules form layers. There are several different types of smectic mesophases. The most important ones are smectic A (SmA), smectic C (SmC) and smectic C* (SmC*). In SmA the director \mathbf{n} is perpendicular to the planes of the layers, whereas in SmC and SmC* the molecules are directed with an angle other than 90° to the plane and direction of molecules varies continuously from layer to layer respectively. The molecules in smectic A are in random position while molecules that form smectic C phase are either a racemic mixture or non-chiral which are randomly positioned within each layer (Dierking, 2003).

Under the observation of polarized optical microscope (POM), SmA appears to be observed as fonic-fan texture whereas SmC and SmC* are observed broken-fan shape and colour when viewed under POM respectively (Dierking, 2003). All smectic phases are layered structures with well-defined layer structured. Motions are restricted within these planes. The texture and molecular arrangement of smectic liquid crystals are shown in Figure 1.8 (a) – (c).

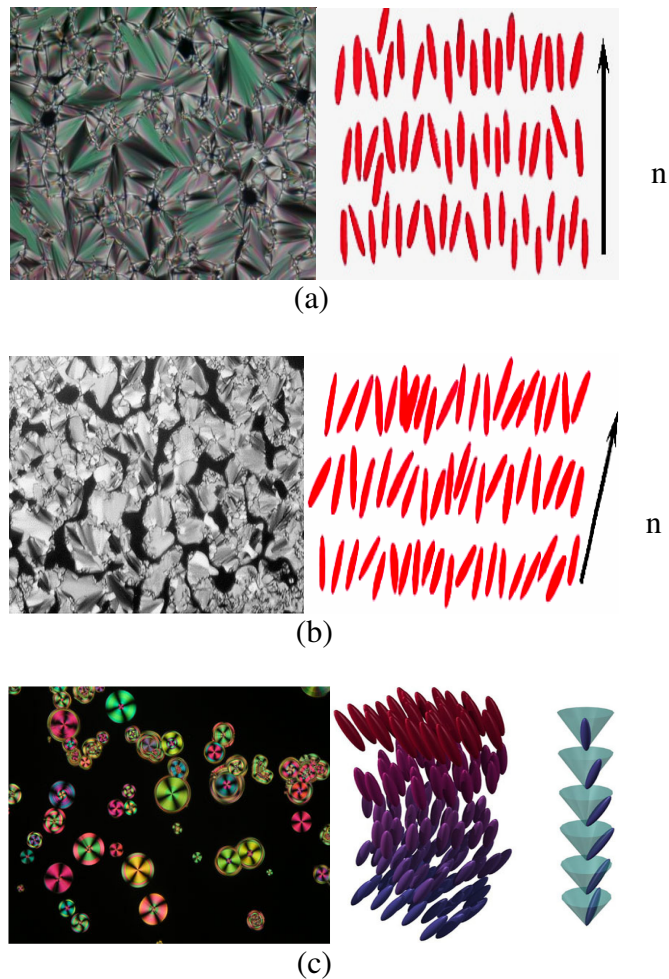


Figure 1.8: (a) Texture and molecular arrangement of typical smectic A liquid crystal. (b) Texture and molecular arrangement of typical smectic C liquid crystal. (c) Texture and molecular arrangement of typical smectic C* liquid crystal

iii) Cholesteric Phase

The cholesteric or known as chiral nematic is a liquid crystal phase is typically composed of nematic mesogenic molecules containing a chiral centre which produces intermolecular forces that favour alignment between molecules at a slight angle to one another. This leads to the formation of a structure which can be visualized as a stack of very thin 2-D nematic-like layers with the director in each layer twisted with respect to those above and below (Plc.cwru, 2010).

The molecules shown are merely representations of the many chiral nematic mesogens lying in the slabs of infinitesimal thickness with a distribution of orientation around the director. Figure 1.9 shows the texture and molecular arrangement of cholesteric liquid crystals (Plc.cwru, 2010).

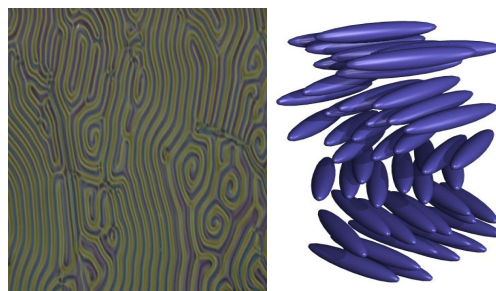


Figure 1.9: Texture and molecular arrangement of typical cholesteric liquid crystal

1.3 Applications of Liquid Crystals

Since year 1968, growth of liquid crystal starts rapidly. Now, it is expanded encompass new areas such as fiber optic communications, new versions of twisted nematic display, nematic devices, polymer dispersed in liquid crystal devices and others. It becomes apparent as the liquid crystalline compound is found to have ability to detect extremely small changes in temperature, mechanical stress, electromagnetic radiation and chemical environment (Fisch, 2006).

The most common application of liquid crystal technology is liquid crystal displays (Figure 1.10). This field has grown into a multi-billion dollar industry, and many significant scientific and engineering discoveries have been made. A liquid crystal display (LCD) is a thin, flat electronic visual display that uses the light modulating properties of liquid crystals (LCs). LCs does not emit light directly. They are used in a wide range of applications, including computer monitors, television, instrument panels, aircraft cockpit displays, signage, etc. They are common in consumer devices such as clocks, watches, calculators, and telephones. LCDs have displaced cathode ray tube (CRT) displays in most applications. They are available in a wider range of screen sizes than CRT and plasma displays, and since they do not use phosphors, they cannot suffer image burn-in (Wikipedia, 2010).

Besides that, liquid crystals also applied in making thermometer (Figure 1.10). This is due to chiral nematic (cholesteric) liquid crystals reflecting light with a wavelength equal to the pitch. Because the pitch is dependent upon temperature, the colour reflected also is dependent upon temperature. Liquid crystals make it possible to accurately gauge temperature just by looking at the colour of the thermometer. By mixing different compounds, a device for practically any temperature range can be built (Wikipedia, 2010).

In addition of that, more important and practical applications have been developed in such diverse areas as medicine and electronics. Special liquid crystal devices can be attached to the skin to show a "map" of temperatures. This is useful because often physical problems, such as tumours, have a different temperature than the surrounding tissue. Liquid crystal temperature sensors can also be used to find bad connections on a circuit board by detecting the characteristic higher temperature (Collings *et al.*, 1998).

An application of liquid crystals that is only now being explored is optical imaging and recording. In this technology, a liquid crystal cell is placed between two layers of photoconductor. Light is applied to the photoconductor, which increases the material's conductivity. This causes an electric field to develop in the liquid crystal corresponding to the intensity of the light. The electric pattern can be

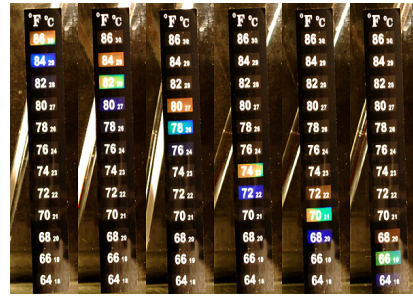
transmitted by an electrode, which enables the image to be recorded. This technology is still being developed and is one of the most promising areas of liquid crystal research (Wikipedia, 2010).

Liquid crystals have a multitude of other uses. They are used for non-destructive mechanical testing of materials under stress. This technique is also used for the visualization of radio frequency (RF) waves in waveguides. They are used in medical applications where, for example, transient pressure transmitted by a walking foot on the ground is measured. Low molar mass (LMM) liquid crystals have applications including erasable optical disks, full colour "electronic slides" for computer-aided drawing (CAD), and light modulators for colour electronic imaging (Wikipedia, 2010).

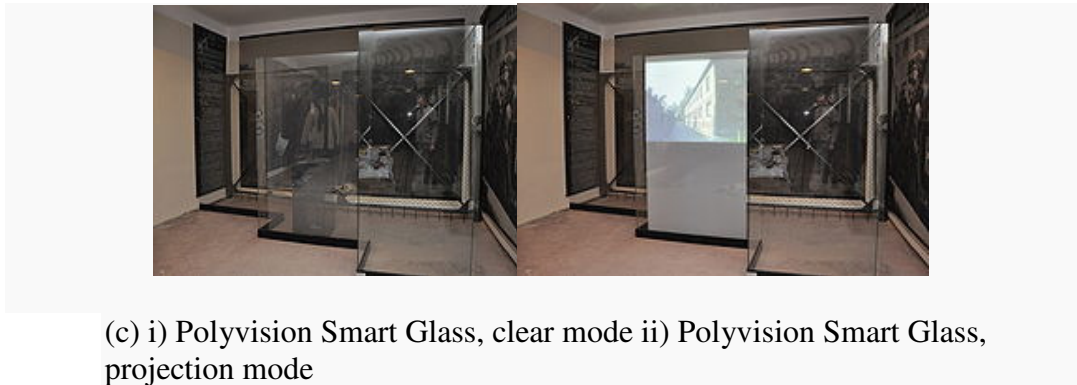
As new properties and types of liquid crystals are investigated and researched, these materials are sure to gain increasing importance in industrial and scientific applications.



(a) Liquid Crystal Display



(b) Liquid Crystal Thermometers



(c) i) Polyvision Smart Glass, clear mode ii) Polyvision Smart Glass, projection mode



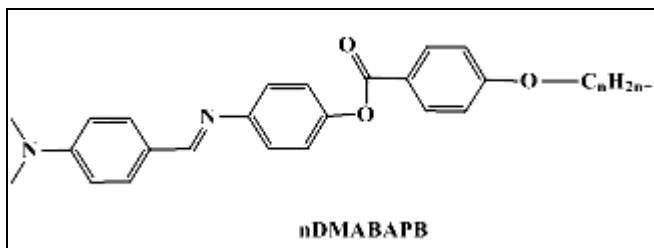
(d) Liquid crystal tuneable filters

Figure 1.10: Some of the application of liquid crystals

1.4 Objectives

The main objectives of this project are:

1. To synthesis 4-((4-(dimethylamino)benzylidene)amino)phenyl-4-alkanoyloxybenzoate, **nDMABAPB**, where $n=10, 12, 14, 16$ and 18 .



2. To characterise the structure of the synthesized compounds by using FTIR, NMR and MS.
3. To determine the liquid crystalline properties of the synthesized compounds by using DSC and POM.

CHAPTER 2

LITERATURE REVIEW

2.1 Schiff Base Liquid Crystals

Schiff base has been received overwhelming response in liquid crystals research ever since in 1970 where Kelker discovered the 4-methoxybenzylidene-4'-butylaniline (MBBA) which exhibit nematic phase at room temperature (Yeap *et al.*, 2006). Now, MBBA is used as a standard in liquid crystal in most investigated nematic compound research. Schiff base is a functional group which consist a carbon-nitrogen double bond with the nitrogen atom connected to an alkyl or aryl group but not with the hydrogen. The general formula of a typical Schiff base are $R_1R_2C=N-R_3$, where R_3 is the alkyl or aryl group which make the Schiff base a stable imines. Imines can be form by aromatic amine react with a carbonyl compound by nucleophilic addition with forming a hemiaminal first and followed by dehydration process. For better illustration, Figure 2.1 shows the mechanism of imine formation.

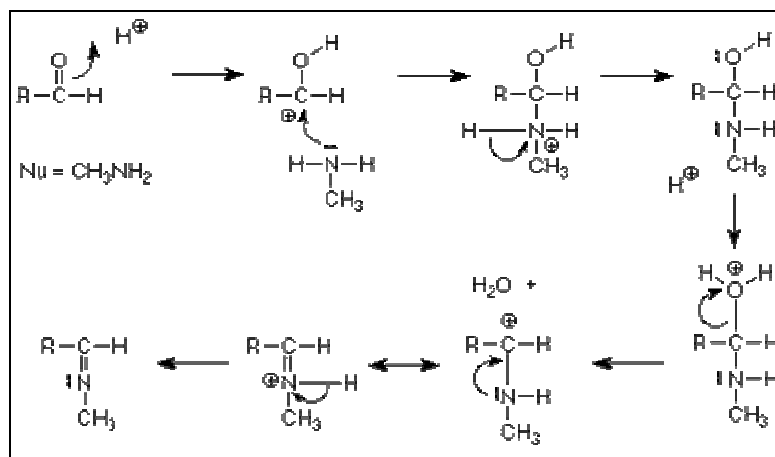


Figure 2.1: Mechanism of imine formation (Chemistry2.csudh, 2011)

In liquid crystal studies, Schiff base has been used as the linking group where the phase transition temperature and physical properties changes are contributed mainly by the linking group. Though it provides a stepped core structure, it maintains molecular linearity, hence providing higher stability and enabling mesophase formation (Collings *et al.*, 1998). Schiff bases are very useful in liquid crystal research because of its rich polymorphism and convenience due to low temperature of phase transitions (Galewski, 1994). In addition, two or more alkoxy chains Schiff bases with longer chains will be expected to exhibit better polymorphism.

2.2 Structure-Mesomorphic Properties Relationship

In liquid crystals studies, structure of a compound is essential to determine a compound possess any mesomorphic properties or not. The specific combination of the structural moieties can confer certain morphology phases and to determine the physical properties of the materials. Based on the most scientist reported, mesophases are mostly exhibit when a compound contain a rigid core, long side chains and rod-like molecules packed in a parallel manner.

2.2.1 Influence of Terminal Group on Mesomorphic Properties

Series of elongated azomethine esters containing two aromatic rings with stearyl moiety as one of the terminal carbon chain with various substituents, X at the other end of molecule have been reported by Ha *et al.*, 2010. The substituents X = H, F, Cl, Br, OCH₃, CH₃ and C₂H₅. The structure of the final compounds is shown as Figure 2.2 below:

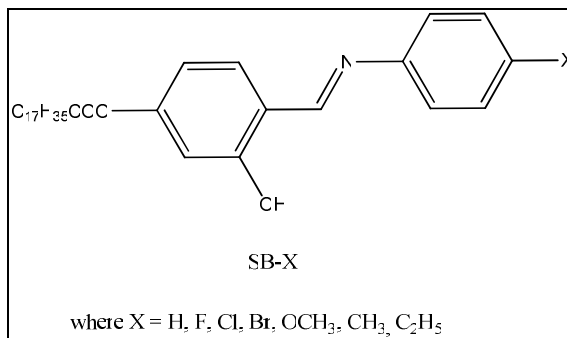


Figure 2.2: Structure of 3-hydroxy-4-[[4-X-substitutedphenyl)imino]methyl}phenyloctadecanoate (Ha *et al.*, 2010)

Different substituents (X) at the *para* position of the aniline fragment were found to exert an effect on the mesomorphic properties. Compounds with halogen and methoxy substituents (X= F, Cl, Br, OCH₃) exhibited liquid crystal phases, whereas the compounds with less polar substituents, X = CH₃, C₂H₅ are appeared as non-mesomorphic derivatives (Ha *et al.*, 2010).

This can be explained as the oxygen of methoxy (OCH₃) group being in conjugation with the aromatic core, which extending the length of the rigid core, enhances the polarizability whereas the CH₃ is more shorter length compared to methoxy and thus does not exhibit any mesomorphic properties (Ha *et al.*, 2010).

Whereas for compounds **SB-ME** (-CH₃) and **SB-ET** (-C₂H₅), which possess methyl and ethyl group in the respective aniline fragment, do not exhibit mesomorphic properties. This might cause by the introduction of the hydroxyl

group in the *ortho* position causes the mesophase stability to favour for terminal chains of shorter length. As such, the compound with short terminal length is expected to possess a higher degree of molecular order, which is favoured by the increase in the polarizability (Ha *et al.*, 2010).

The influence of terminal group on mesophase stability can be considered as one of the factors contributing towards the difference of temperature for transition from mesophase to isotropic phase. Among compounds **SB-X** (where X = F, Cl and Br), wherein each compound possesses the halogen in the aniline fragment, the clearing temperature for compound **SB-F** (-F) is very much lower in comparison with **SB-CL** (-Cl) and **SB-BR** (-Br). This comparison suggests that the fluorine (F) atom, which is the most electronegative, reduces the degree of molecular order despite the presence of hydroxyl group at *ortho* position. This thermal data also indicates that the influence of steric hindrance caused by the asymmetry of the central core of compound **SB-F** (F) is the least in comparison with compounds **SB-CL** (-Cl) and **SB-BR** (-Br), which possess higher clearing temperatures (Ha *et al.*, 2010).

2.2.2 Influence of Core group on Mesomorphic Properties

Three series of ω -unsaturated compounds Phm, Bm and PhBm consists a linear perfluorinated chain and differing rigid cores were reported by Fornasieri *et al.* (2003). The structures for the three series are shown as Figure 2.3 below:

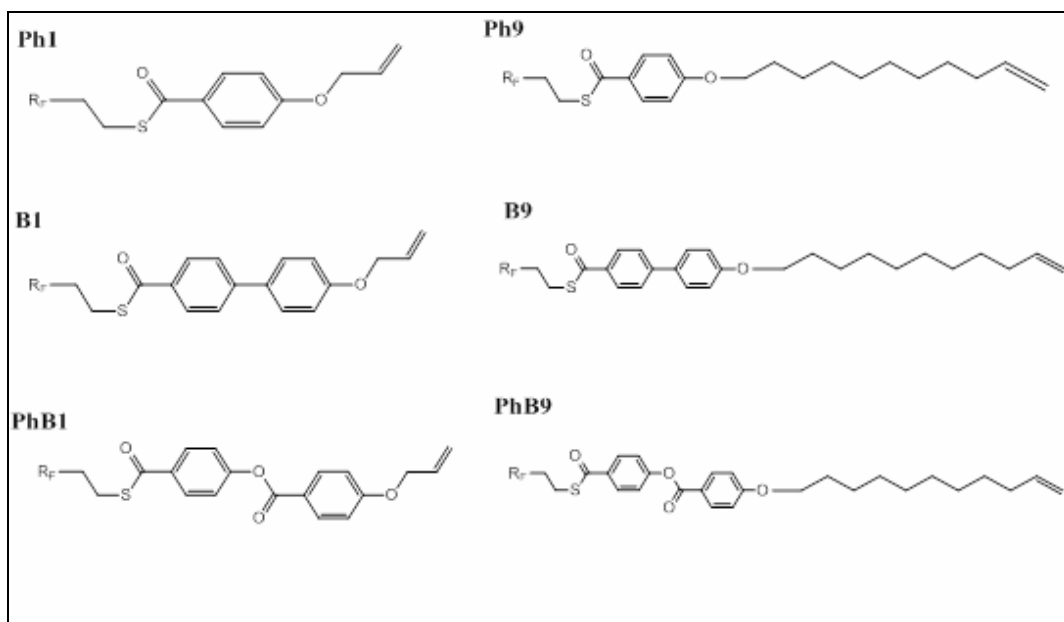


Figure 2.3: Structures of series Phm, Bm, Phbm ($m=1, 9$, $R_F=C_6F_{13}$)

Based on the research carried, increasing of the aromatic rings on the core structures of a liquid crystal compounds can largely affected on the transition temperature of that particular compound. Increasing the number of rings resulted in increasing in transition temperature as well. This can further shown as the Table 2.1 below which indicated the transition temperatures of the ω -unsaturated derivatives (Fornasieri *et al.*, 2003).

Table 2.1: Overall transition temperatures measured on heating for the ω -unsaturated derivatives. Cr, SmX, SmA, and I indicate crystal, smectic X, smectic A, and isotropic phases respectively.

Compound	Transition Temperature, °C					
	Cr		SmX		SmA	I
Ph1	•	29.3			• 97.8	•
Ph9	•	50.3			• 51.7	•
B1	•	138.5			• 226.6	•
B9	•	111.7	•	152.8	• 158.8	•
PhB1	•	36.3			• 217.6	•
PhB9	•	62.8	•	138.0	• 148.8	•

Within the allyloxy series (Ph1, B1, PhB1) the monophenyl group gives mesomorphic transitions at lower temperatures in comparison with the homologues containing two aromatic rings. In the journal, the monophenyl allyloxy derivative shows interesting smectogenic enantiotropic character near room temperature. Besides that, from the DSC curves which obtained from the journal, Ph1 exhibits a mesophase spanning approximately 68°C on heating and more than 100°C on cooling. This indicated that the compound requires strong supercooling to crystallize and it remains for at least twelve hours in the mesophase at room temperature. The key to obtaining these impressive physical properties is the presence of the thioester functionality. The biphenyl core (B1) leads to the shift of the mesophase to higher temperatures but with the temperature range unchanged whereas phenyl benzoate group actually stabilizes the mesophase at wider range (181°C). B1 and PhB1 exhibit high clearing temperatures

accompanied by structure modifications and thus are irreversible (Fornasieri *et al.*, 2003).

2.2.3 Influences of Alkyl Chain Length on Mesomorphic Properties

In a recent work by Ha *et al.*, 2010, a homologous series of Schiff base esters, 4-chlorobenzylidene-4'-n-alkanoyloxyanilines, containing even number of carbons at the end groups of the molecules ($C_{n-1}H_{2n-1}COO-$, $n = 4, 6, 8, 10, 12, 14, 16$) were reported. The structures of the compounds are shown as Figure 2.4 below:

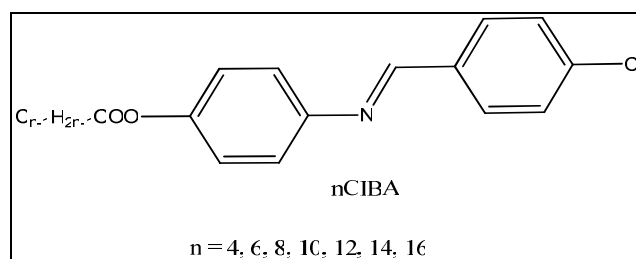


Figure 2.4: 4-chlorobenzylidene-4'-n-alkanoyloxyanilines, nCIBA (Ha *et al.*, 2010).

n-butanoyloxy having the shortest alkyl chain length was appeared to be non-mesogenic. However, there were three exotherms were observed for n-hexanoyloxy during cooling cycle and this suggested that the presence of two mesophases in this compound. Whereas, for higher members of the series, n-octanoyloxy to n-hexadecanoyloxy it showed that two endotherms in the DSC

thermograms which can be attributed to the isotropic liquid to mesophase and mesophase-crystal transitions (Ha *et al.*, 2010).

When increasing in length of terminal chain, the homologous series changed from non mesogenic to monotropic and eventually changed to enantiotropic properties. For n-butanoyloxy (C4), the core system is too rigid and hence, it is hard for it to form mesophase. Meanwhile, the packing of molecules in hexanoyloxy (C6) tends to be less rigid compared to n-butanoyloxy, thus it showing monotropic properties. As from n-octanoyloxy (C8) to n-hexadecanoyloxy (C16), the homologous members showed enantiotropic properties. This is mainly because the increase number of carbons enhances the flexibility of the chain and subsequently promotes enantiotropic phase. In addition, the melting points of the final compounds are gradually decreased from C4 to C16 due to the dilution of core system (Ha *et al.*, 2010).

As reported by Swager *et al.*, 2007, ionic liquid crystals with different core sizes and imidazolium group for lateral substitution have been synthesized. The general structures of the compounds are as Figure 2.5 below:

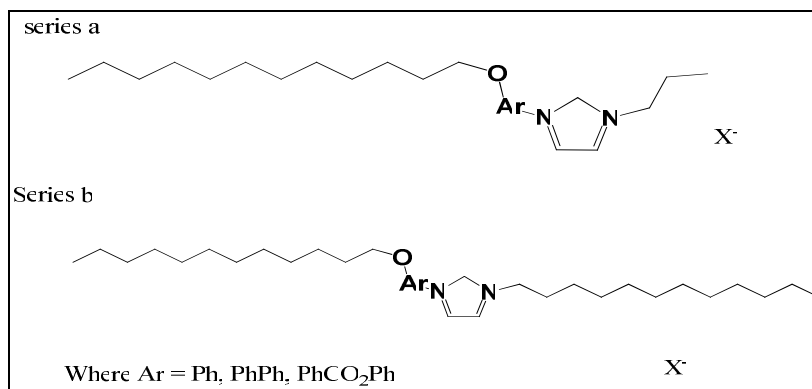


Figure 2.5: General structures of the ionic liquid crystals with different core sizes and imidazolium group for lateral substitution

There is different in transition temperatures of four groups of ionic liquid crystals with cores differentially substituted with: series (a) propyl substituents and (b) dodecyl substituents. An increase in the core size by the introduction of an ester group between the two phenyl rings results in a decreased range of Sm A stability due to an increase in the melting temperatures. In addition, all of the prepared esters display polymorphism at low temperatures with up to three crystal phases. A decreased core size obtained by omitting one of the phenyl rings has a large effect on the mesomorphic properties. For the propyl-substituted material, the clearing temperature drops significantly to 57 °C and the corresponding BF₄⁻ salt does not exhibit liquid crystalline properties. By increasing the tail length from propyl to dodecyl or trimethyldodecyl, stable mesophases are obtained, but the clearing temperatures remain much lower (Swager *et al.*, 2007).

2.2.4 Influence of Lateral Substituents on Mesomorphic Properties

Figure 2.6 below shown the three series of Schiff base ester, 2-hydroxy-4-methoxybenzylidene-4'-alkanoyloxyaniline (series A), 2-hydroxy-3-methoxybenzylidene-4'-alkanoyloxyaniline (series B) and 3-methoxy-4-alkanoyloxybenzylidene-4'-alkanoyloxyaniline (series C), which possess mono- and di-substituted moieties at both ends of the molecules with alkanoyloxy chains $n= 12, 14, 16,$ and $18,$ have been reported by Yeap *et al.* (2006).

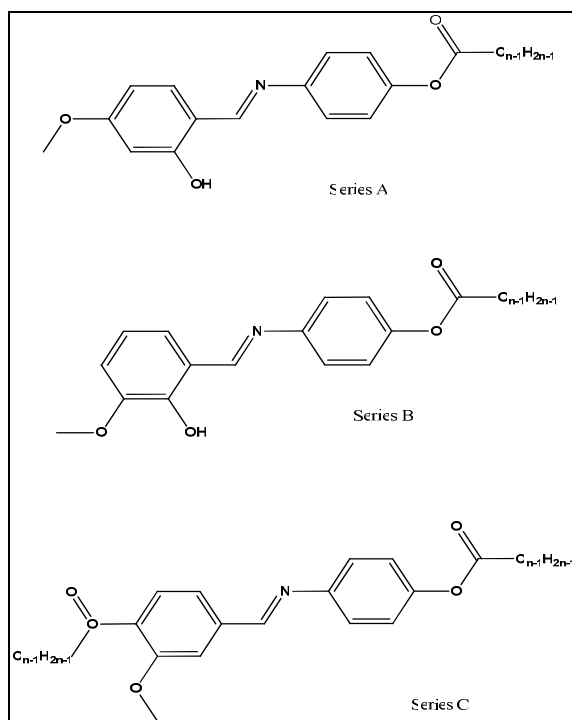


Figure 2.6: Structures of 2-hydroxy-4-methoxybenzylidene-4'-alkanoyloxyaniline (Series A), 2-hydroxy-3-methoxybenzylidene-4'-alkanoyloxyaniline (series B) and 3-methoxy-4-alkanoyloxybenzylidene-4'-alkanoyloxyaniline (series C) upon heating (Yeap *et al.*, 2006).

In the reported journal, series A, it is clear that it stated that all the compounds were exhibit endotherms characteristic of the crystal-mesophase and mesophase-isotropic transition at temperatures greater than the melting temperature (T_m) upon heating. Observation by polarized optical microscope also suggested that during heating and cooling, the Nematic phase appeared in all the compounds (Yeap *et al.*, 2006).

Meanwhile, in series B, all the derivatives appeared to be non mesogenic. This happened even the supercooling of these compounds failed to produce a monotropic mesophase. These could happen mainly because introduction of the lateral methoxy substituent at meta-position in series B is more unfavourable to form mesophases compared with the series A which the substituent are attached at para-position. This might mainly cause by introduction the lateral methoxy substituent at meta-position exerts a molecular broadening influence, reducing the lateral intermolecular force of attraction and thus impeding liquid crystal formation. For series C, smectic C phase appeared with broken fan-shaped texture under the observation of polarized optical microscope during supercooling suggested that isotropic-mesophase transition occurred (Yeap *et al.*, 2006).

In summary, the mesogenic homologous series (**A**, **B** and **C**) containing a Schiff's base core with lateral methoxy and hydroxy groups indicates that the molecular broadening caused by the *meta*-methoxy group in the aldehyde fragment

of 2-hydroxy-3-methoxybenzalidene-4'-alkanoyloxyanilines (series **B**) suppresses the thermal stabilities of mesophases, leading to the formation of non-mesogenic materials whereas the introduction of the carbon side chain at the para-position in the aldehyde fragment the increase of molecular length-breadth ratio, which seemed to outweigh the broadening effect caused by the *meta*-methoxy group. In order to generate a smectic phase (SmA or SmC) in the analogous substituted $C_6H_5CH = NC_6H_5$ compounds, the number of carbons in the terminal alkyl chain ($C_{n-1}H_{2n-1}COO-$) must be at least 18 ($n \geq 18$) of which all compounds in the homologous series **A** exhibited an enantiotropic N phase except for compound **A18** (with $n = 18$) which exhibited an enantiotropic SmA phase. Compounds in the homologous series **C**, with both side chains (wherein $2n \geq 24$) along the long molecular axis, exhibited a monotropic SmC phase (Yeap *et al.*, 2006).

Two series of semi-fluorinated chiral liquid crystals, 2F($m = 8-12$) and 3F($m = 8-12$), with monofluoro-substitution at the 2- and 3-positions of the first phenyl ring near the chiral chain, respectively, have been reported in Wu *et al.* (2004). The structures for the two series compounds can be represent by the Figure 2.7 below:

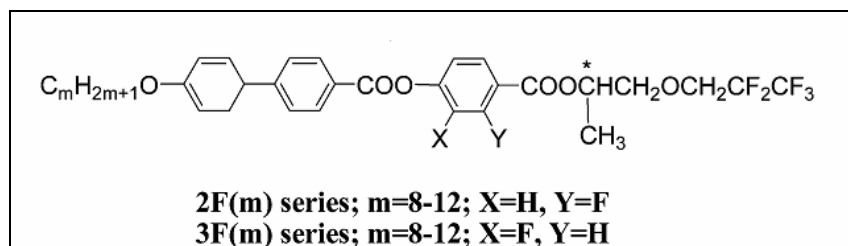


Figure 2.7: Structure of (R)-2-Fluoro-4-[1-methyl-2-(2,2,3,3,3-pentafluoropropoxy)ethyloxycarbonyl]phenyl 4'-alkyloxybiphenyl-4-carboxylates(**2F**) and (R)-3-Fluoro-4-[1-methyl-2-(2,2,3,3,3-pentafluoropropoxy)ethyloxycarbonyl]phenyl 4'-alkyloxybiphenyl-4-carboxylates(**3F**), where ($m = 8-12$)

In the series $2F(m = 8-12)$ compounds, it was found that $2F(m = 8)$ and $2F(m = 10)$ exhibit broad temperature ranges which is 125°C and 88°C , respectively where it is of the SmC^*_A phase and have the phase sequence $\text{SmA}^* - \text{SmC}^* - \text{SmC}^*_A$. However, in the series $3F(m = 8-12)$, a direct $\text{SmA}^* - \text{SmC}^*_A$ transition accompanied by a higher order ferroelectric SmX^* phase was found in compounds $3F(m = 8-10)$. The remainder have the phase sequence $\text{SmA}^* - \text{SmC}^*$. It is worth noting that the anti-ferroelectric SmC^*_A phase was reported to occur generally in compounds with alkyl chain length from $m = 8$ to 10 for these materials. It is also found that as the fluoro substituent moves from the 2- to the 3- position of the phenyl ring, the mesophase transition temperatures of $\text{I} - \text{SmA}^*$ and $\text{SmA}^* - \text{SmC}^* / \text{SmC}^*_A$ transitions decrease, suggesting that the 2-fluoro substituent is more sterically shielded and molecular broadening is minimized (Wu *et al.*, 2004)

CHAPTER 3

MATERIALS AND METHODOLOGY

3.1 Chemicals

The chemicals used throughout the project were listed as below:

1. Chemicals were obtained from Merck, Germany:
 - a) 1-Bromodecane
 - b) 1-Bromododecane
 - c) 1-Bromotetradecane
 - d) 1-Bromohexadecane
 - e) 1-Bromooctadecane
 - f) 4-Aminophenol
 - g) N,N'-Dicyclohexylcarbodiimide (DCC)
 - h) 4-(Dimethylamino)-pyridine (DMAP)

2. Chemicals were obtained from Sigma-Aldrich, Germany:
 - a) Ethyl-4-hydroxybenzoate

3. Chemicals were obtained from Fisher Scientific, United Kingdom:
 - a) Potassium Carbonate

4. Chemicals were obtained from R&M Marketing, United Kingdom:
 - a) Potassium Hydroxide
 - b) Hexane
 - c) Dichloromethane (DCM)

5. Chemicals were obtained from BDH Chemical, England:
 - a) 4-Dimethylaminobenzaldehyde
 - b) Dimethylformamide (DMF)

6. Chemicals were obtained from Prochem, United States of America:
 - a) Acetone

7. Chemicals were obtained from Scharlau Chemie S.A., Europe Union:
 - a) Ethanol

3.2 Instruments

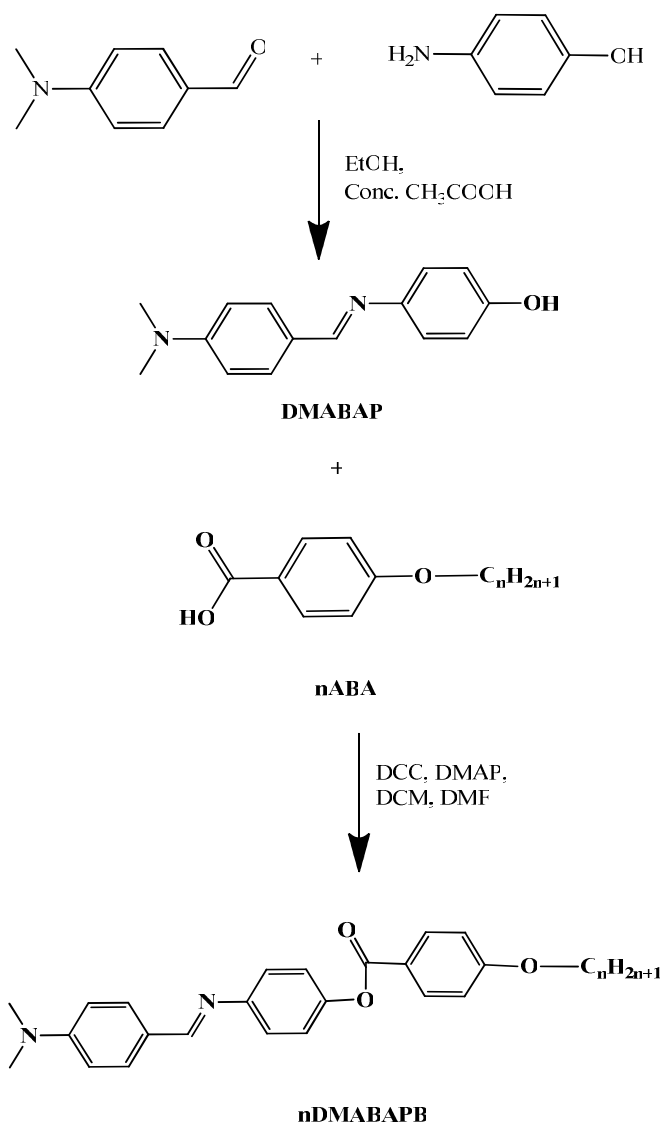
During the project was carried, several instruments were used to characterise the properties of the compounds which synthesised. The types of models, functions and the venues where the instruments located are listed in Table 3.1 as below:

Table 3.1: List of Instruments used in this Project

Types of models	Functions	Locations
Perkin Elmer 2000-FTIR Spectrometer (Spectrum RX1)	Identify useful structural information and reference to generalise characterisation of functional group frequencies.	UTAR, Kampar
Stuart SMP10 Melting Point Apparatus	Determine the melting point and melting ranges of compounds.	UTAR, Kampar
Mettler Toledo DSC823 Differential Scanning Calorimeter	To determine the enthalpy changes and the mesophase existences of compounds.	UTAR, Kampar
NMR Spectrometer Joel JNM-ECX400	To identify the molecular structure and dynamic of compounds.	UTAR, Kampar
Carl Zeiss Polarising Optical Microscope equipped to Linkam Scientific Instruments LTS350	To investigate the mesophase that possess of the products synthesised.	USM, Penang
Electron Ionisation Mass Spectrometer (EI-MS) Finnigan MAT95XL-T spectrometer	To identify the m/z values of compounds synthesized.	NUS, Singapore

3.3 Synthesis

The synthesis route towards the formation of **nDMABAPB** shown in Figure 3.1



where $n = 10, 12, 14, 16$ and 18

Figure 3.1: Reaction scheme of intermediate **DMABAP** and final compound, **nDMABAPB**

3.3.1 Synthesis of 4-((4-(dimethylamino)benzylidene)amino)phenol, DMABAP

Equimolar of 4-dimethylaminobenzaldehyde (5 mmol, 0.75 g) and 4-aminophenol (5 mmol, 0.54 g) was weighed into separated beakers. Beaker that contained 4-aminophenol, ethanol (40 mL) was added. The mixture was heated until dissolved. Then, the solution was filtrated into the beaker with 5 mmol of 4-dimethylaminobenzaldehyde. Concentrated acetic acid (5 drops) was added. The mixture was stirred for two hours. The yellowish precipitate formed was then collected by suction filtration and put into an oven to dry.

3.3.2 Synthesis of 4-(alkanoyloxy)benzoic acid, nABA

Ethyl-4-hydroxybenzoate (5 mmol, 0.83 g) and potassium carbonate (5 mmol, 0.69 g) were weighed respectively into a same round-bottom flask with acetone (40 mL) added to the flask and start reflux with stirring. After the mixture started reflux, 1-bromododecane (5 mmol) was added into the mixture and continued reflux for 24 hours. Then, the mixture was filtered into another round-bottom flask and allowed to heat until all the acetone solvent dried. Ethanol (40 mL) was added with excess of KOH. The mixture was allowed to reflux for 5 hours. Then, the mixture was cooled to room temperature. Concentrated of hydrochloric acid (few drops) were then added and shaken slowly. White

precipitate was formed. Small amount of distilled water then was added. Suction filtration was done for the mixture. The precipitate collected was stored in oven dried. The steps above were repeated with 1-bromoalkane where carbon chains n=12, 14, 16 and 18 respectively.

3.3.3 Synthesis of 4-((4-(dimethylamino)benzylidene)amino)phenyl-4-(alkanoyloxy)benzoate, nDMABAPB

3.3.3.1 Synthesis of 4-((4-(dimethylamino)benzylidene)amino)phenyl-4-(decyloxy)benzoate, 10DMABAPB

DMABAP (1 mmol, 0.239 g) was dissolved in a soluble amount of dimethylformamide, DMF. 4-(decyloxy)benzoic acid (1mmol), dimethylaminopyridine (1 mmol), DMAP and dicyclohexylcarbodiimide (1 mmol), DCC were dissolved in sufficient amount of dichloromethane (DCM).

All the materials were mixed into a 100 mL round bottom flask. The reaction was stirred at 0 °C for an hour and followed by five hours stirring at room temperature. Cloudy light yellowish solid was observed during the stirring process.

The solution then filtered with a filter paper through aided of a separating funnel. Cloudy yellowish solid was found as the residue whereas the filtrate was in clear light yellowish solution. The filtrate was then air dried overnight. Light yellowish solid was formed and the solid formed was crystallized with hexane and followed by ethanol to obtained pure final compound. The final compound then dried in an oven with 50 °C. The final compound was transferred and weighed. The percentage yielded was 40.56 %

3.3.3.2 Synthesis of 4-((4-(dimethylamino)benzylidene)amino)phenyl-4-(dodecyloxy)benzoate, 12DMABAPB

All the procedures as stated for **10DMABAPB** was applied to synthesise 4-((4-(dimethylamino)benzylidene)amino)phenyl-4-(dodecyloxy)benzoate, **12DMABAPB** except 4-(dodecyloxy)benzoic acid, **12ABA** was replaced the 4-(decyloxy)benzoic acid, **10ABA**. The percentage yielded was 46.67 %.

3.3.3.3 Synthesis of 4-((4-(dimethylamino)benzylidene)amino)phenyl-4-(tetradecyloxy)benzoate, 14DMABAPB

All the procedures as stated for **10DMABAPB** was applied to synthesize 4-((4-(dimethylamino)benzylidene)amino)phenyl-4-(tetradecyloxy)benzoate, **14DMABAPB** except 4-(tetradecyloxy)benzoic acid, **14ABA** was replaced the 4-(decyloxy)benzoic acid, **10ABA**. The percentage yielded was 52.89 %.

3.3.3.4 Synthesis of 4-((4-(dimethylamino)benzylidene)amino)phenyl-4-(hexadecyloxy)benzoate, 16DMABAPB

All the procedures as stated for **10DMABAPB** was applied to synthesize 4-((4-(dimethylamino)benzylidene)amino)phenyl-4-(hexadecyloxy)benzoate, **16DMABAPB** except 4-(hexadecyloxy)benzoic acid, **16ABA** was replaced the 4-(decyloxy)benzoic acid, **10ABA**. The percentage yielded was 56.87 %.

3.3.3.5 Synthesis of 4-((4-(dimethylamino)benzylidene)amino)phenyl-4-(octadecyloxy)benzoate, **18DMABAPB**

All the procedures as stated for **10DMABAPB** was applied to synthesize 4-((4-(dimethylamino)benzylidene)amino)phenyl-4-(octadecyloxy)benzoate, **18DMABAPB** except 4-(octadecyloxy)benzoic acid, **18ABC** was replaced the 4-(decyloxy)benzoic acid, **10ABA**. The percentage yielded was 60.56 %.

3.4 Characterisation

3.4.1 Infrared Spectral Analysis

Homologous series of 4-((4-(dimethylamino)benzylidene)amino)phenyl-4-(alkanoyloxy)benzoate, **nDMABAPB** were analysed with Perkin Elmer 2000-FTIR (Spectrum RX1) spectrometer at the frequency of 4000-400 cm^{-1} . The sample was prepared in the KBr pellet form. Identification of the functional groups can be done based on the significant peaks at certain frequencies and prediction of the structure of the compounds can be made by using the single beam infrared spectrometer.

3.4.2 Thin Layer Chromatography (TLC)

The analysis was carried by using aluminium-backed silica-gel plates supplied from Merck, Germany and examined under short wave ultraviolet (UV) light. The mobile phase used is mixtures of chloroform and ethyl acetate with the ratio of 2:1.

3.4.3 ^1H and ^{13}C Nuclear Magnetic Resonance (NMR)

NMR Joel JNM-ECX400 was used for analysing the ^1H and ^{13}C NMR spectroscopy of compounds. The samples were pre-dissolved in deuterated chloroform, CDCl_3 at room temperature (298 K). Tetramethylsilane, TMS was used as the internal standard. The final products was tested for ^1H NMR at the range of chemical shift 0.0-10.0 ppm whereas ^{13}C NMR at the range at 0.0-20.0 ppm.

3.4.4 Mass Spectroscopy Analysis (MS)

An electron ionisation mass spectrometry (EIMS) spectrum was obtained by using Finnigan MAT95XL-T spectrometer, with electron ionisation impact in gas phase. The conditions used for the spectrometer is 70 eV electron energy with 200 °C of source temperature.

3.4.5 Differential Scanning Calorimetry (DSC)

Mettler Toledo DSC823 differential scanning calorimeter was used to analyse the enthalpy changes of samples. First, the samples were weighed approximately 1-2 mg and transferred to a 45 µL pure aluminium crucible respectively. Then, crucibles were crimped tightly with cover by using a sealing press.

The sample was then placed into the sample compartment of the DSC instrument. The rate and temperature for both heating and cooling were set accordingly for various samples. The heating and cooling was taken under 1 mL/minutes of nitrogen flow. After the scanning of the sample completed, the sample was removed for the compartment for the next sample.

3.4.6 Polarised Optical Microscopy Analysis

Liquid crystal phase and transition temperature were observed by using Carl Zeiss Polarising Optical Microscope equipped with Linkam Hostage. First, the samples were transferred on the slides and covered with glass cover respectively. Then, the slide was moved into the hot stage. The focus of microscope was adjusted to obtain a maximum resolution. The liquid crystalline textures of the product were observed under a polarizing optical microscope equipped with a hostage and temperature regulator. Then, the slide was removed and ready for the next sample.

CHAPTER 4

RESULTS AND DISCUSSION

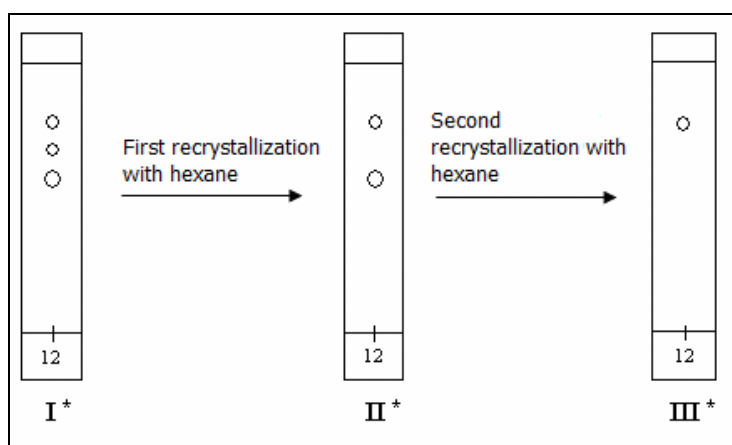
4.1 Structure Elucidation

Structure elucidation of the compounds was established through the spectroscopic method such as FTIR, ^1H NMR and ^{13}C NMR. Purity of intermediate compounds of **DMABAP**, **nABC** ($n = 12, 14, 16$ and 18), and final compounds **nDMABAPB** ($n = 10, 12, 14, 16$ and 18) was confirmed by using the TLC analysis method. **12DMABAPB** and **10ABA** were discussed as the representative cases for FTIR analysis. Spectra for others compounds were expected and give similar pattern as observed for **12DMABAPB** and **10ABA**. Meanwhile **12DMABAPB** and **16DMABAPB** were choosing respectively for NMR and MS analysis.

4.1.1 Thin Layer Chromatographic Analysis

Thin Layer Chromatographic plates spotted with the final product were developed in chloroform: ethyl acetate, 2:1 solvent system. The TLC plates of **12DMABAPB** are shown in Figure 4.1 as a representative for the compounds.

There were three spots obtained after running the first TLC test (**I**), on the pale yellow final product. Upon recrystallization from hexane, the product gave the second TLC plate shown as (**II**), with only two spots. Subsequent recrystallization from another portion of hexane produced TLC plate (**III**), with only one spot. This confirmed that the final product was pure.



* Plates were eluted in a 2:1 ratio of chloroform to ethyl acetate solvent system and visualized under a 254 nm UV light lamp

Figure 4.1: Sketch of TLC plates for **12DMABAPB**

4.1.2 Fourier Transform Infrared Spectroscopy (FTIR) Analysis

4.1.2.1 Infrared Spectral Analysis on 4-((4-

(dimethylamino)benzylidene)amino)phenol, DMABAP

Infrared spectra of starting materials 4-aminophenol and 4-dimethylaminobenzaldehyde, intermediate compound **DMABAP** are shown in Figure 4.2.

The characteristic of 4-aminophenol, **4AP** can be shown by the two strong N-H stretching peaks at 3341 and 3282 cm^{-1} , C-H aromatic stretching indicated by medium broad peak from 2590 to 3031 cm^{-1} , and the strong C=C aromatic stretching peak shown at 1510 cm^{-1} . The characteristic peak of the O-H stretch which predicted should appear as weak peak in the range of 3000 to 3500 cm^{-1} is not obviously seen owing to the overlapping strong peak of the N-H stretch. The two peaks of N-H stretching was mainly due to the 4-aminophenol is a primary amines. The higher frequency peak results form an asymmetric vibration whereas the lower frequency is due to the symmetric vibration.

From the spectrum of the 4-dimethylaminobenzaldehyde, **4DMAB** there are three weak peaks appeared at 2903, 2795, and 2713 cm^{-1} . These peaks are a typical C-H stretching of an aldehyde compound. The medium peak at 1661 cm^{-1} is due to C=O bond. This peak appeared at lower frequency range because of the conjugation of C=O bond with phenyl. Besides that, there are a strong absorption peak and a medium peak at 1594 and 1548 cm^{-1} respectively. These peaks are caused by the aromatic C=C bond in the phenyl group. A strong peak allocated at 1163 cm^{-1} is due to the presence of the C-N stretching.

The formation of intermediate compound, 4-((4-(dimethylamino)benzylidene)amino)phenol, **DMABAP** can be easily traced from the IR spectrum. It can be confirmed with the presence of OH and C=N peaks in the IR spectrum of **DMABAP**. This is due to the formation of Schiff base uses the N-H group of 4-aminophenol, **4AP** and the aldehyde group, CHO of 4-dimethylaminobenzaldehyde, **4DMAB** to form a new bonding between **4AP** and **4DMAB** with C=N linking functional group. With the formation of Schiff base, this eliminates the N-H stretch from appearing in **DMABAP**. Thus, the imination process has taken places in this reaction. In **DMABAP**, the OH stretching was shown at 3433 cm^{-1} with a weak intensity while the C=N stretching is shown at 1661 cm^{-1} .

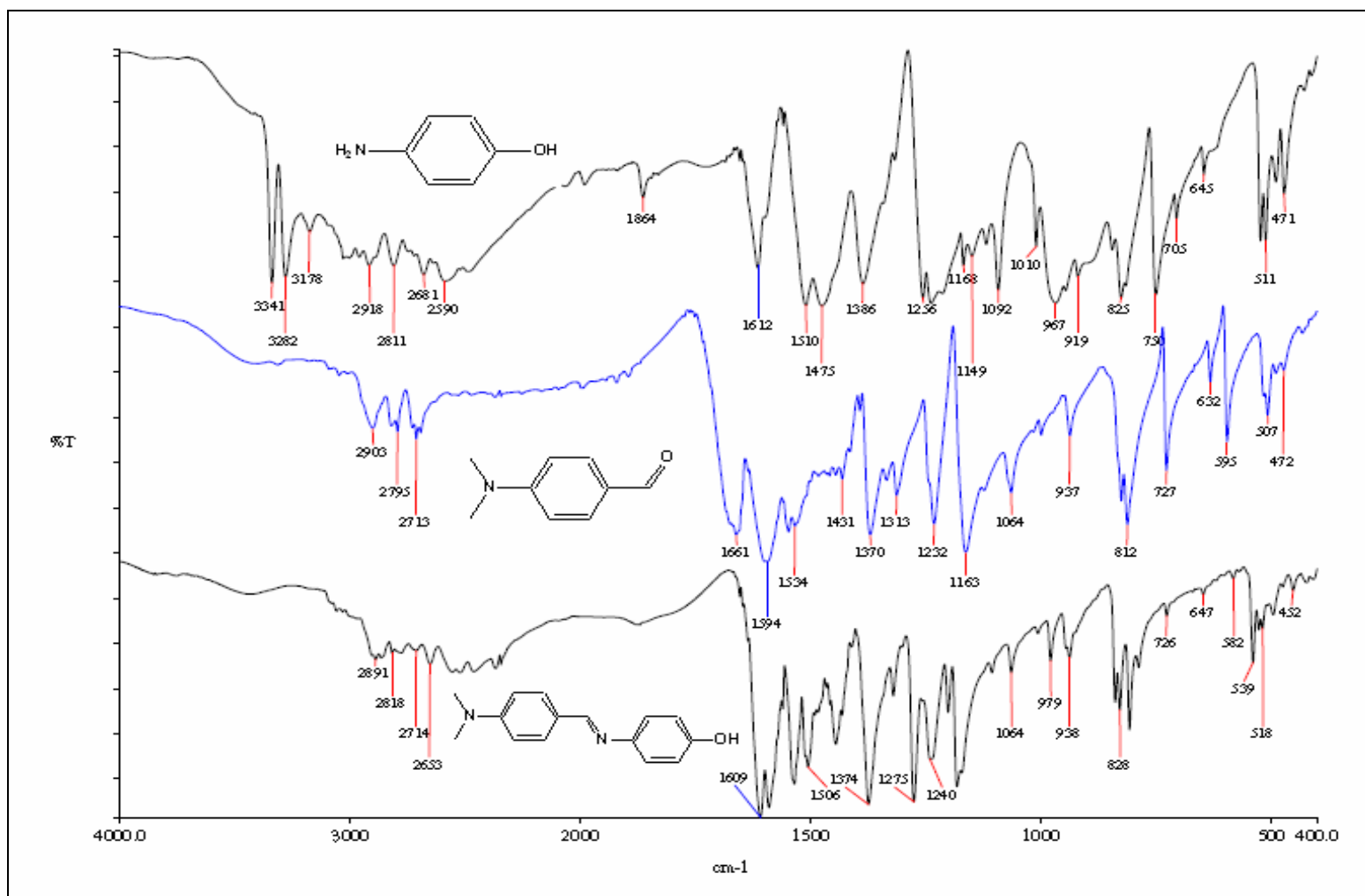


Figure 4.2: IR Spectrums of 4AP, 4DMAB, and DMABAP

4.1.2.2 Infrared Spectral Analysis on n-alkyloxybenzoic acid, nABA

As for the n-alkyloxybenzoic acid intermediates, **nABA**; the FTIR spectrum of 4-(dodecyloxy)benzoic acid, **12ABA** was selected to represent the functional group present. The characteristic of **12ABA** was shown by the presence of sp^3 C-H stretching peak at 2917 and 2850 cm^{-1} , C=O stretching peak at 1686 cm^{-1} , and the C-O stretching peak at 1257 cm^{-1} . This shows the etherification process was successfully done. FTIR spectrum for **12ABA** was shown by Figure 4.3. The data for n-alkyloxybenzoic acid was tabulated in Table 4.1.

Table 4.1 FTIR value for n-alkyloxybenzoic acid, **nABA**

Compound	IR (cm^{-1})			
	C-H sp^2 stretch	C-H sp^3 stretch	C=O stretch	C-O stretch
10ABA	2918s	2851s	1685m	1257s
12ABA	2917s	2850s	1686m	1257s
14ABA	2917s	2850s	1686m	1258s
16ABA	2917s	2850s	1689m	1259s
18ABA	2917s	2849s	1607m	1258s

Note:

M (medium intensity), s (strong intensity)

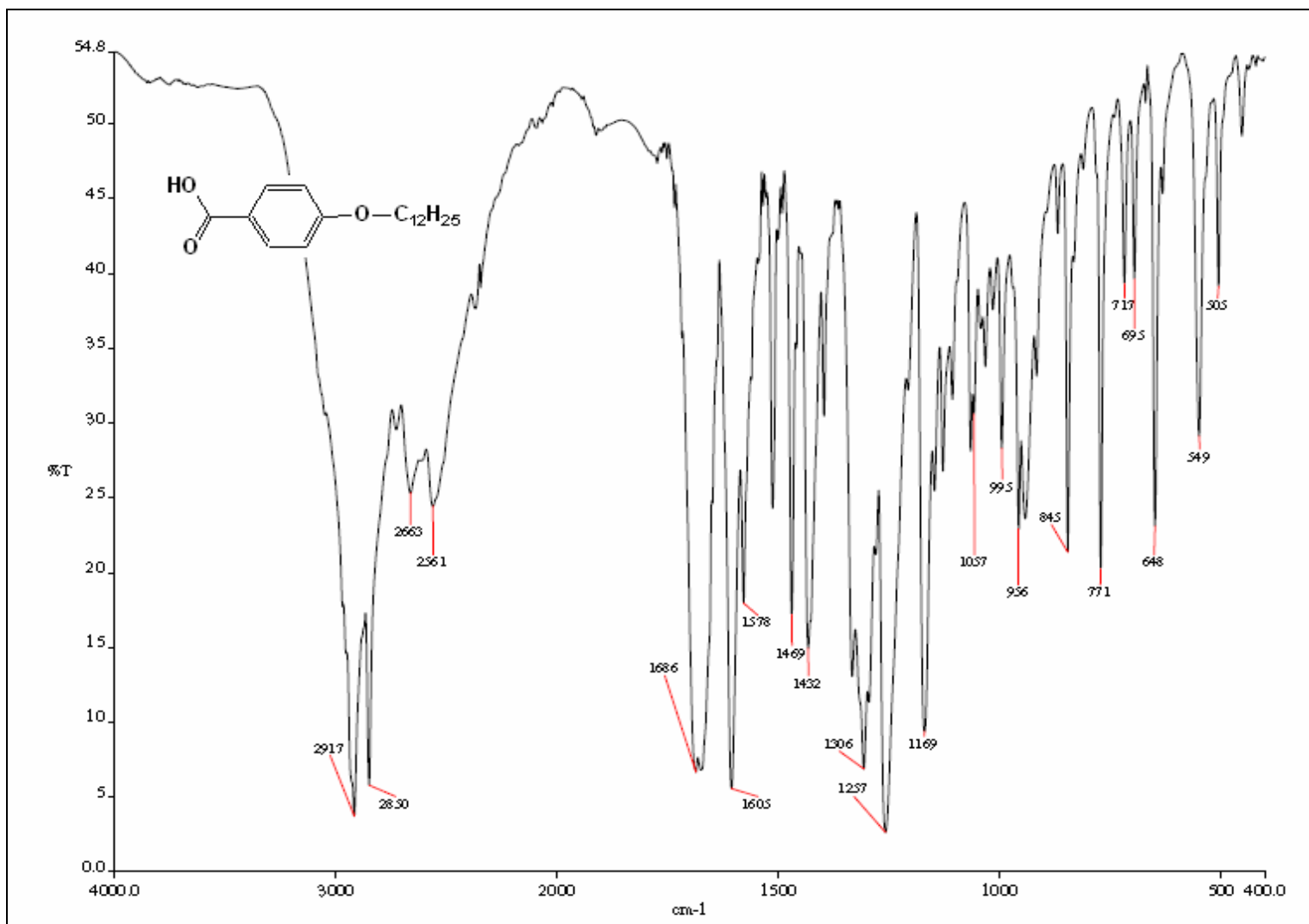


Figure 4.3: FTIR Spectrum of 12ABA

4.1.2.3 Infrared Spectral Analysis on 4-((4-(dimethylamino)benzylidene)amino)phenyl-4-(alkanoyl)benzoate, **nDMABAPB**

In Figure 4.4, the FTIR spectrum shows the formation of Schiff base ester, 4-((4-(dimethylamino)benzylidene)amino)phenyl-4-(dodecyloxy)benzoate, **12DMABAPB** which is formed by the esterification of 4-((4-(dimethylamino)benzylidene)amino)phenol, **DMABAP** and 4-(dodecyloxy)benzoic acid, **12ABA** is shown by the formation of sp^2 C-H stretching peak at 2922 cm^{-1} and sp^3 C-H stretching peak at 2848 cm^{-1} , C=O stretching peak at 1724 cm^{-1} , and C-O stretching at 1250 cm^{-1} which is all shown in strong intensity. The formation of ester functional group which are C=O and C-O between 4-((4-(dimethylamino)benzylidene)amino)phenol, **DMABAP** and 4-(dodecyloxy)benzoic acid, **12ABA** shows the esterification is successfully performed. The FTIR data of **nDMABAPB** was tabulated in Table 4.2.

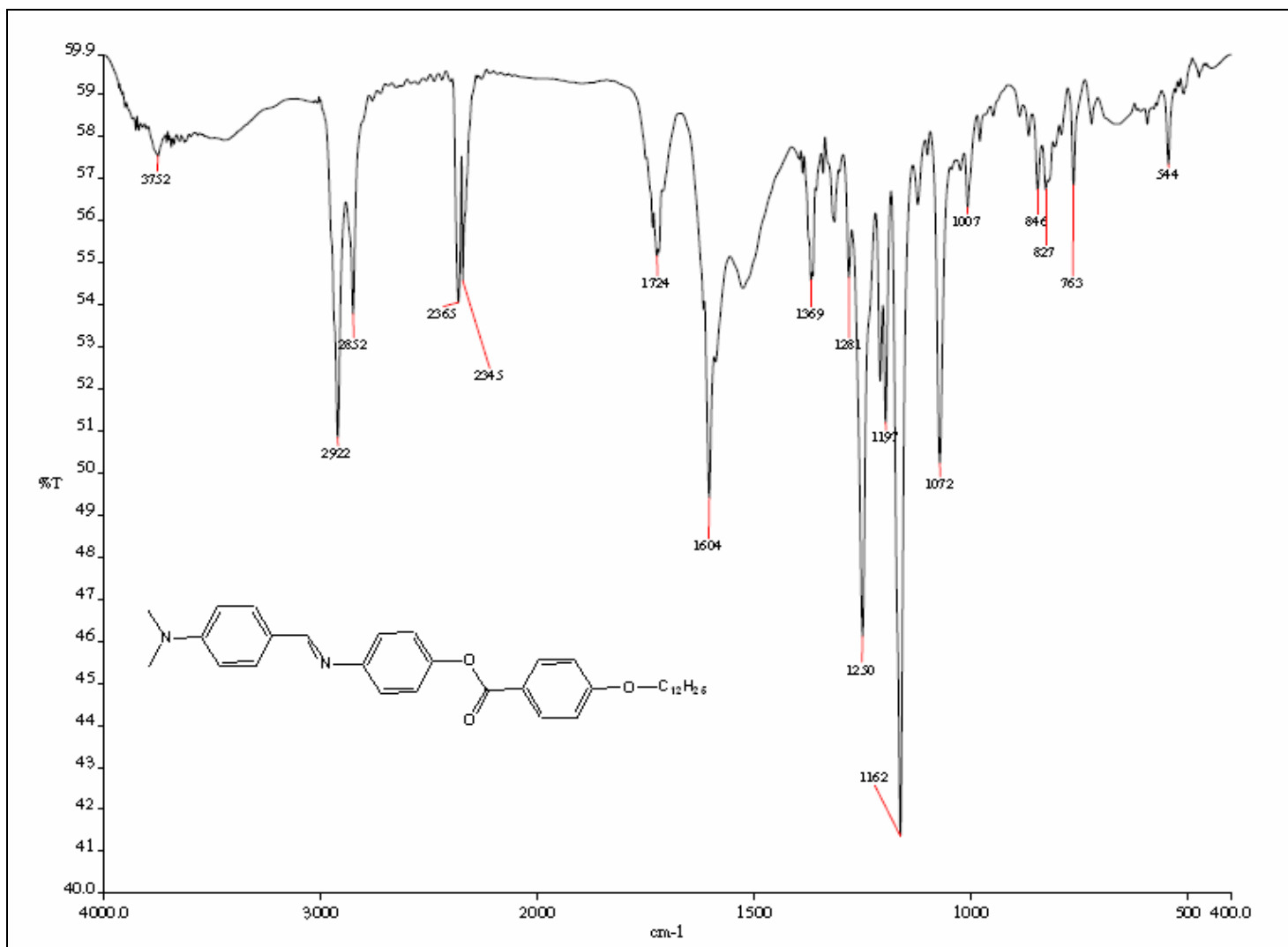


Figure 4.4: IR Spectrum of 12DMABAPB

Table 4.2: FTIR data for **nDMABAPB**

IR (cm ⁻¹)	Compound				
	10DMABAPB	12DMABAPB	14DMABAPB	16DMABAPB	18DMABAPB
C-H sp ² stretch	2923m	2922m	2923s	2922s	2919s
C-H sp ³ stretch	2848m	2848m	2848s	2851s	2851s
C=O stretch	1734w	1724w	1724w	1734w	1734m
C=N stretch	1604m	1604m	1601m	1604s	1605s
C-O stretch	1257s	1250s	1256s	1255s	1256s
1,4-disubstituted aromatic ring	846w	846w	846w	846w	848w

Note:

w (weak intensity), m (medium intensity), s (strong intensity)

Based on Figure 4.5, the comparison of infrared spectrum of the starting material **4AP**, intermediate **DMABAP** and final product **12DMABAPB** is shown clearer whereby FTIR data was tabulated in Table 4.3.

Table 4.3: FTIR value for **4AP**, **DMABAP** and **12DMABAPB**

IR (cm ⁻¹)	Compound		
	4AP	DMABAP	12DMABAPB
O-H stretch	-	3448	-
N-H stretch	3341, 3290	-	-
C=N stretch	-	1609	1604m
C=C stretch	1513	1590	-
C-H aromatic	2483-3034	2524-2891	-
C-O stretch	1238	1275	1250s
C-H sp ² stretch	-	-	2922m
C-H sp ³ stretch	-	-	2848m

Note:

w (weak intensity), m (medium intensity), s (strong intensity)

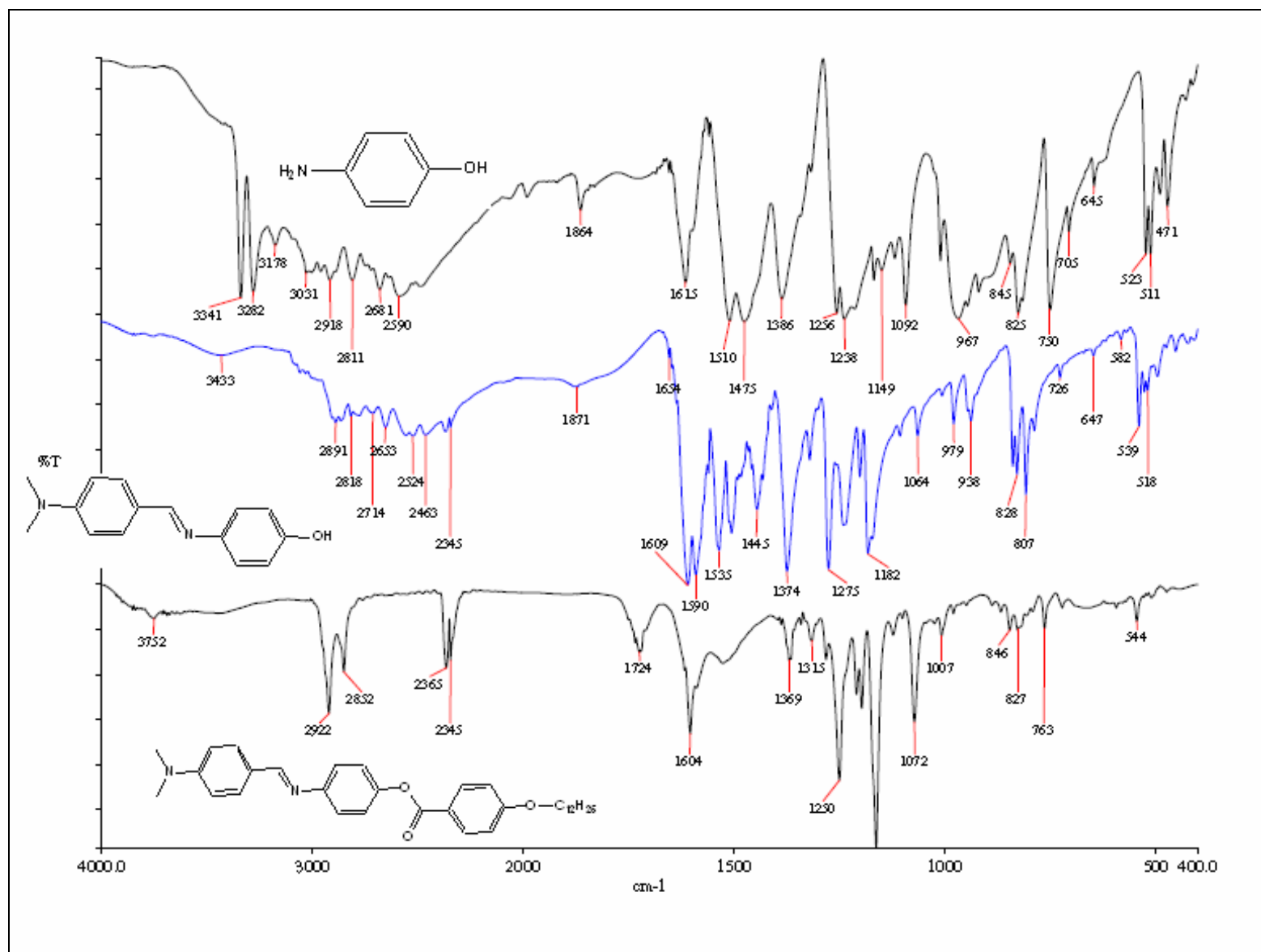


Figure 4.5: Comparison of FTIR of 4AP, DMABAP and 12DMABAPB

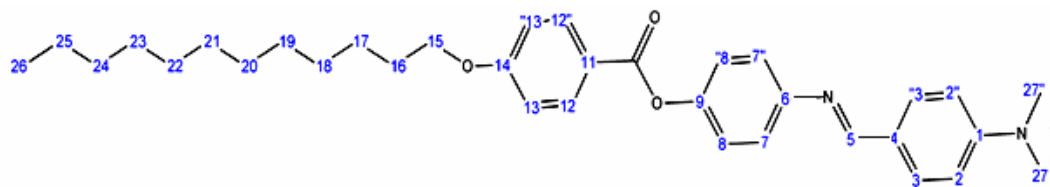
4.1.3 Nuclear Magnetic Resonance (NMR) Analysis

4.1.3.1 ^1H NMR Spectra Analysis on 4-((4-

(dimethylamino)benzylidene)amino)phenyl-4-(dodecyloxy)benzoate,
12DMABAPB

12DMABAPB is chosen as the representative to discuss and interpret the results of the ^1H NMR spectrum obtained (Figure 4.6). The molecular structure of the **12DMABAPB** with its numbering scheme is shown in Table 4.4.

Table 4.4: ¹H NMR data and the proposed structure of **12DMABAPB**



Proton Assigning	Chemical Shift, δ (ppm)	Multiplicity
H26	0.86-0.95	Triplet
H17-H25	1.23-1.60	Multiplet
H16	1.77-1.89	Quintet
H27, H27'	3.06-3.15	Singlet
H15	3.95-4.10	Triplet
H2, H2'	6.68-6.78	Doublet
H13, H13', H8, H8'	6.90-7.03	Quartet
CDCl ₃	7.20-7.30	Singlet
H7, H7', H3, H3'	7.72-7.80	Doublet
H12, H12'	8.09-8.19	Quartet
H5	9.75-9.80	Singlet

The most upfield triplet signals appeared at $\delta = 0.86-0.95$ ppm was caused by the methyl protons at the end of the long alkyl chain which the three protons are chemically and magnetically equivalent. These hydrogens in the methyl groups (H32) are the most highly shielded type of proton and therefore shown the NMR

signal at the lowest chemical shift. Meanwhile, the multiplet signals at $\delta=1.23-1.60$ ppm were owned to the methylene protons, H23-31 present. As quintet signals appeared at $\delta= 1.77-1.89$ ppm is typically due to proton, H21. This because based on the (n+1) rules, which 2 adjacent protons from the H20 and H23 respectively affecting the splitting and induced the quintet splitting. For the most intense singlet signal at approximately $\delta= 3.06-3.15$ ppm is due to the two methyl groups protons, H33 and H34 from the $-\text{N}(\text{CH}_3)_2-$. Whereas at the region $\delta = 3.95-4.10$ ppm, triplet signal were detected. This is mainly caused by the H20 because the two adjacent protons from the H21 has obeyed the (n+1) rules and give rise to triplet splitting.

As for the most deshielded singlet signal appeared at $\delta= 9.75-9.80$ ppm region was due to proton of imine linking group, H5 (Yeap et al., 2006a, 2006b, 2006c).The signal appeared as singlet is mainly because there are no adjacent protons. Existence of sp^2 hybridisation in double bond and electron withdrawing effect of nitrogen atom shifted the H8 to the most downfield. There were few signals appeared at $\delta=6.69-8.19$ ppm region are mainly due to the presence of three aromatics rings. The doublet signals shown at the chemical shift $\delta= 8.09-8.19$ ppm is because of the aromatic protons of H16, H18 and H10, H14 while the chemical shift at $\delta= 7.72-7.80$ ppm is due to the aromatic protons of H15 and H19. The quartet signals show at $\delta= 6.90-7.03$ ppm are caused by the H2, H6 and H3, H5 respectively. While as for the chemical shift of $\delta= 6.68-6.78$ ppm are due to the aromatic protons of H11, H13.The oxygen presence with its electron withdrawing

effect has affected the chemical shift of H16, H18 and H10, H14 higher than the H15, H19 and H11, H13 respectively which indicated by electronegativity of oxygen atoms. Besides that, as for the nitrogen has lower electronegativity compared to oxygen, its electron-withdrawing effect in H2, H6 and H11, H13 are weaker than oxygen and thus caused the chemical shift for protons near nitrogen atoms are more likely much lower than near oxygen atoms.

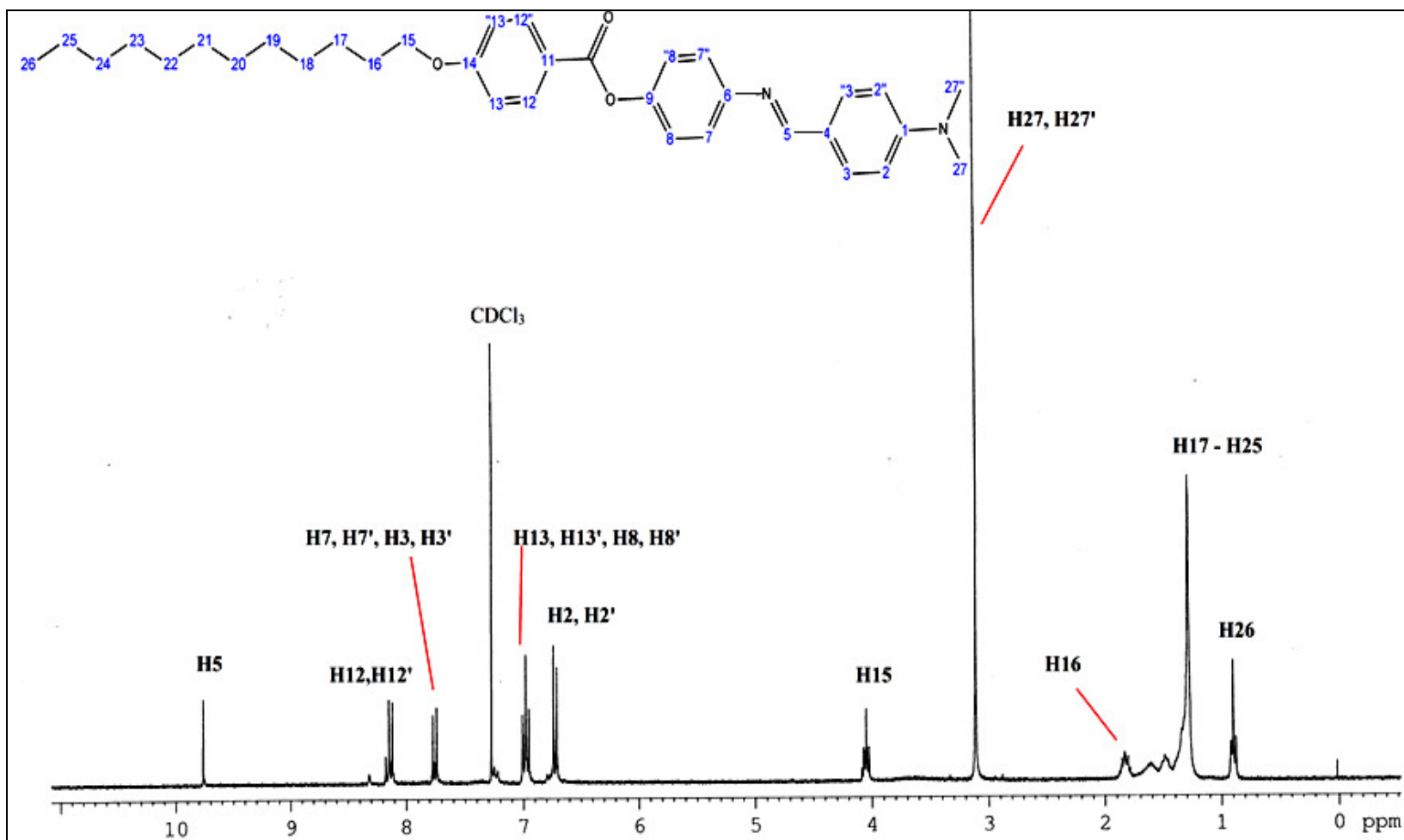


Figure 4.6: ¹H-NMR spectrum of 12DMABAPB

4.1.3.2 ^{13}C NMR Spectra Analysis on 4-((4-(dimethylamino)benzylidene)amino)phenyl-4-(hexadecyloxy)benzoate, **16DMABAPB**

The structures of the synthesized compounds are elucidated by using ^{13}C NMR analysis technique as well. The representative compound for elucidate is **16DMABAPB** (Figure 4.7). Its molecular structure with numbering is shown in Table 4.5 with the tabulated data.

The signal appears at the most low field region at $\delta = 165.8$ ppm is due to the carbonyl group, C=O at C11. This followed by the signal appeared at $\delta = 163.6$ ppm is assigned to imine carbon, C=N at C6. This is because both oxygen and nitrogen are the electronegative atoms in the compound which causing the electron pulling away from the carbon and shifted both C11 and C6 to the most down field in spectrum.

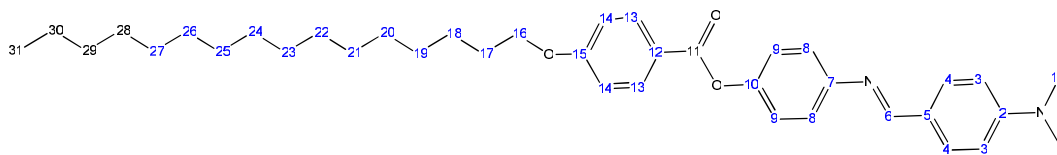
The signals appeared at the low field region in between $\delta = 111.2$ - 158.8 ppm in fact attributed by the aromatic carbons. The aromatic carbon attached to a double bond and thus deshielded due to sp^2 hybridization and diamagnetic anisotropy. Amongst all the aromatic carbons, C6, C2, C7, and C10 are having the lowest intensity. This is mainly due to these four carbons are ipso carbon which is without hydrogen as the substituent directly attached (Pavia *et al.*, 2001). Thus, these four carbons have

relatively weak signals due to a long relaxation time and a weak nuclear overhauser enhancement (NOE) effect.

The chemical shift at $\delta = 68.6$ ppm is assigned to C16. This carbon is relatively low field compared to long alkyl chain because it is directly bonded to an oxygen atom which can act as an electron withdrawing atom and causes the chemical shift lower compared to the alkyl chain. Meanwhile, for the chemical shift at $\delta = 40.6$ ppm is attributed to the C1 and C1'. The nitrogen atom act as the electron withdrawing group has shifted these two carbon to the lower field than the carbon attached to long alkyl chain. The intensity of this peak is resulting from the two equivalent carbon combined the effect together. However, NOE effect also applied to this condition (Pavia, 2001).

The signals appeared to be at the most high field in the spectrum is the more shielded carbon. At the region from $\delta = 14.4-32.2$ ppm, the carbons that contributed to these signals at the region is mainly the carbon atoms that attached to the alkyl chain. The long alkyl chain having a signal which is the strongest intensity among that region due to the NOE effect and the interaction of spin-spin dipoles operates through space (Pavia, 2001).

Table 4.5: ^{13}C NMR data and the proposed structure of **16DMABAPB**



Carbon Assigning	Chemical Shift, δ (ppm)
C11	165.8
C6	163.6
C15	158.8
C2	154.6
C7	144.3
C10	143.5
C13,C13'	132.6
C4,C4'	132.3
C12	122.7
C9,C9'	121.9
C8,C8'	115.9
C5	114.6
C3,C3'	114.4
C14,C14'	111.2
CDCl_3	77.3
C16	68.6
C1,C1'	40.6
C29	32.2
C18-C28	29.9-29.6
C17	26.2
C30	22.9
C31	14.4

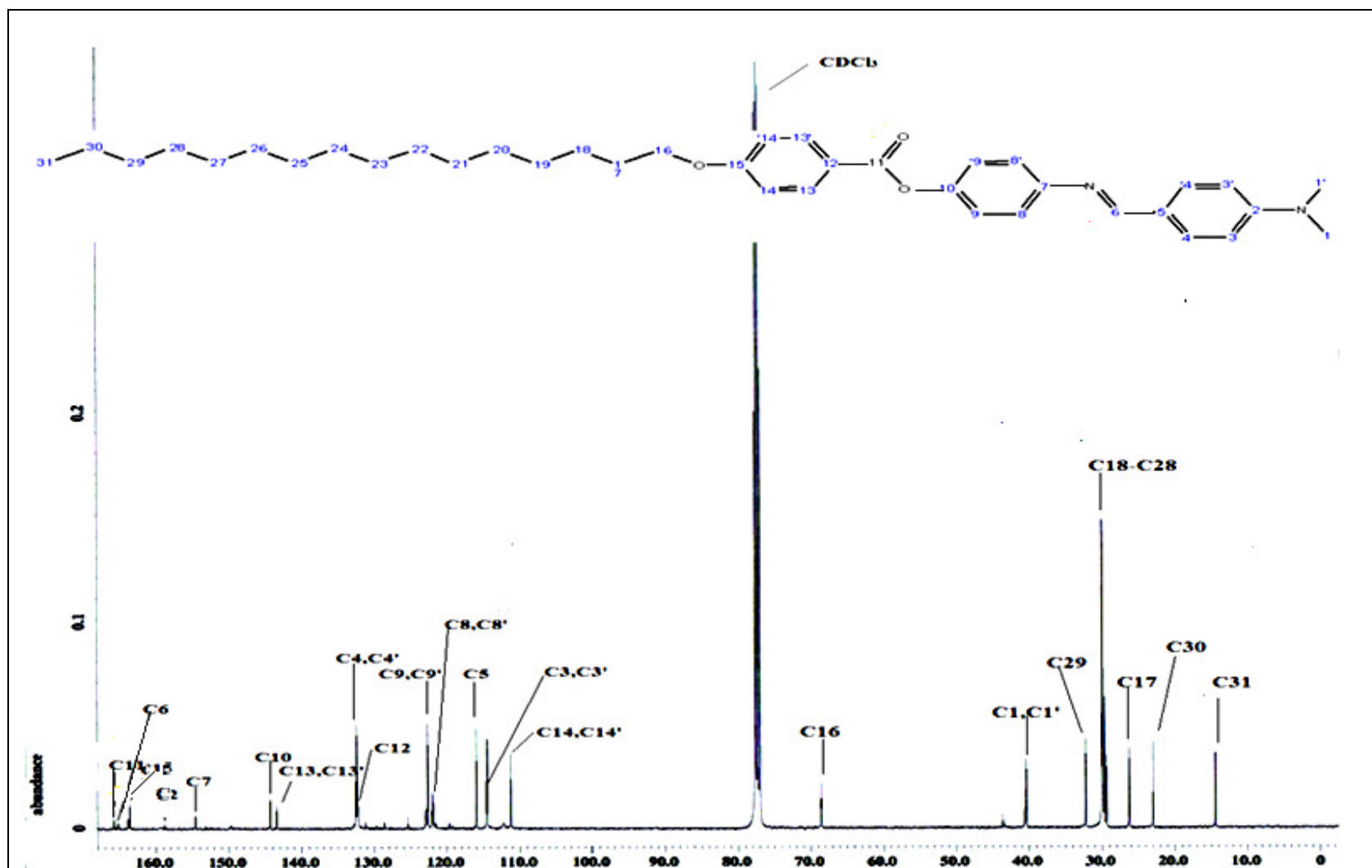
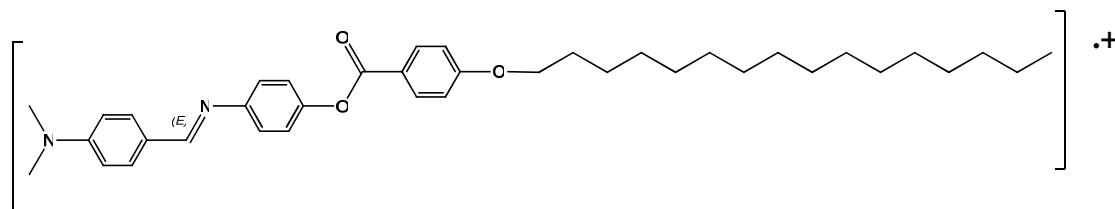


Figure 4.7: ¹³C NMR spectrum of 16DMABAPB

4.1.4 Mass Spectrometry Analysis of 4-((4-(dimethylamino)benzylidene)amino)phenyl-4-(hexadecyloxy)benzoate, **16DMABAPB**

The structure and the purity of the synthesized compound are elucidated by using EI-Mass Spectrometry analysis technique. The structure of the respective compound, **16DMABAPB** (Figure 4.8) with the m/z values and the proposed fragments of the compound are tabulated in Table 4.6

Molecular ion peak, M^+ for **16DMABAPB** is distinguishable. It appears at $m/z = 584.5$.



The beam of electrons in the ionization chamber converts some of the sample molecules to positive ions. The simple removal of an electron from a molecule yields an ion which is the actual molecular weight of the original molecules. The ion is the molecular ion M^+ . From the structure of proposed for **16DMABAPB**, the molecular weight is 584.5 g/mol. Thus, by comparing the theoretical m/z value for molecular ion

M^+ and the mass spectrum of the **16DMABAPB**, the value was matched and further confirmed its structure.

First of all, the α -cleavage on the molecular ion produces the acylium and the phenoxy ion respectively. As the result of cleavage, the peak found at $m/z= 345.3$ in the spectrum of **16DMABAPB**, represents the stable acylium in which the relative abundance is 63.7. As consecutive fragmentation, acylium ion is undergo β -cleavage by eliminating the long alkyl chain, $[C_{16}H_{33}]^+$. It is giving rise highest relative abundance base peak at $m/z= 121.0$. Another ion fragment from α -cleavage, the phenoxy ion is giving rise the peak at $m/z= 267.1$, relative abundance of 63.7.

Finally, there are a medium intensity peak appear at lower m/z in the mass spectrum. This peak most probably due to the fragmentation of the long alkyl chain from 4-(hexadecyloxy)benzoic acid. The m/z value for that particular peak is 43.1 which indicated the present of $C_3H_7^+$.

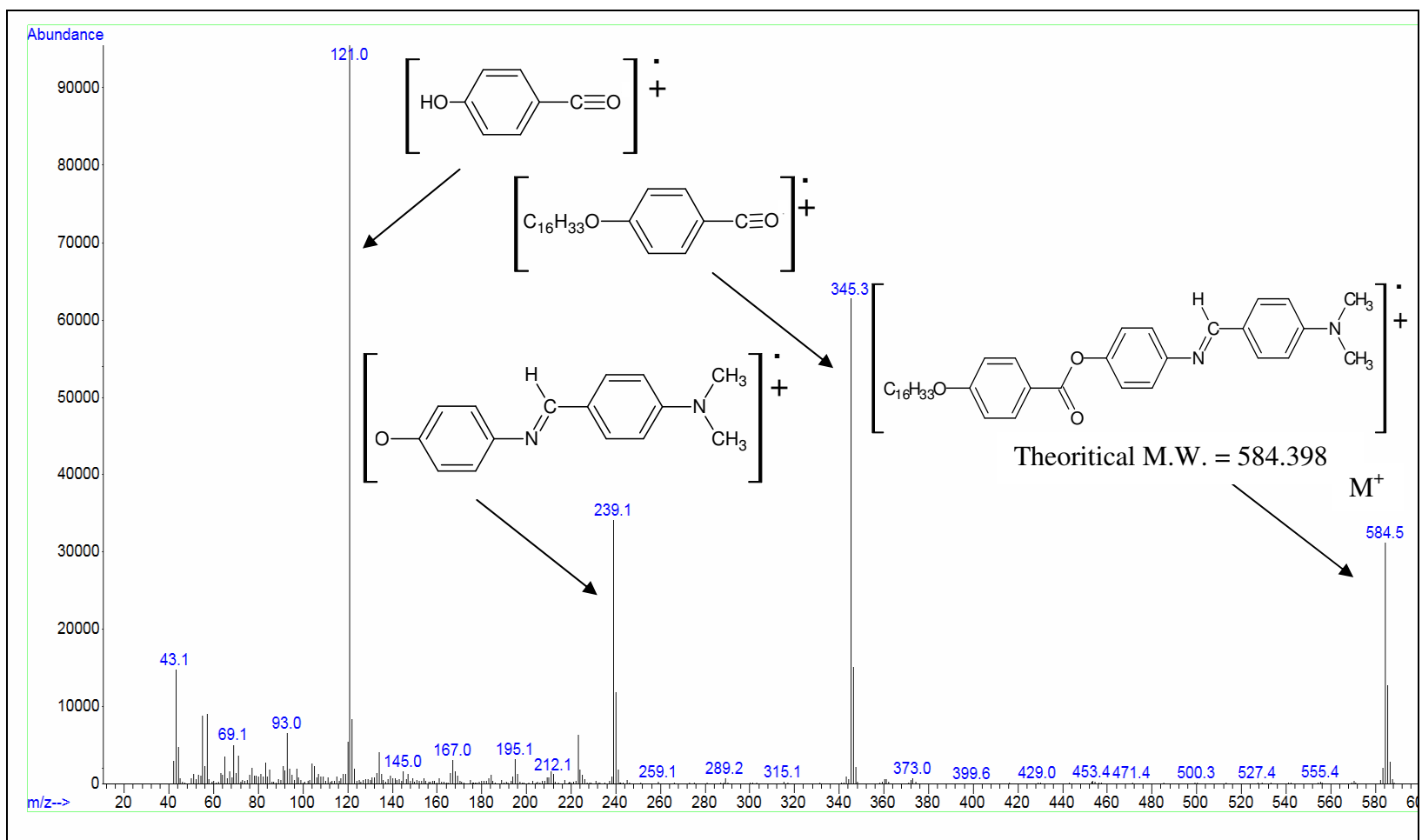
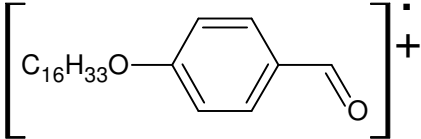
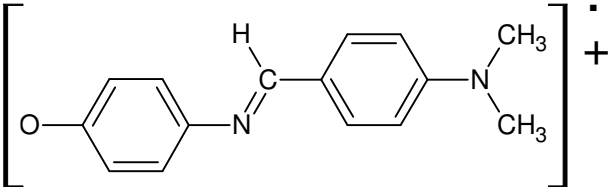
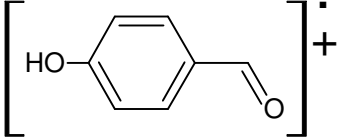


Figure 4.8: Mass Spectrum of 16DMABAPB

Table 4.6: Mass Spectrometry data of **16DMABAPB**

m/z	Relative abundance	Corresponding ion fragment
584.5	31.5	M ⁺
345.3	63.7	
239.1	34.5	
121.0	100.0	

4.2 Mechanism of Steglich Esterification

Steglich Esterification has been successful occurred in between **DMABAP** and various types of benzoic acid. The structures of **nDMABAPB** are confirmed by using FTIR, NMR and Mass Spectroscopy analysis. Below is the proposal mechanism for the esterification which is discussed in Figure 4.9 and 4.10. DCC is a dehydrating agent used mainly for esterification. N,N'-dicyclohexylurea (DHU) is the by-product of DCC combine with the H₂O molecule. DCC promotes the

formation of DHU by converting the carboxyl OH group into a better leaving group (Smith, 2002). However, there is limitation of the use of DCC, that is the yield maybe variable and N-acylureas produced are side-products (Smith, 2000).

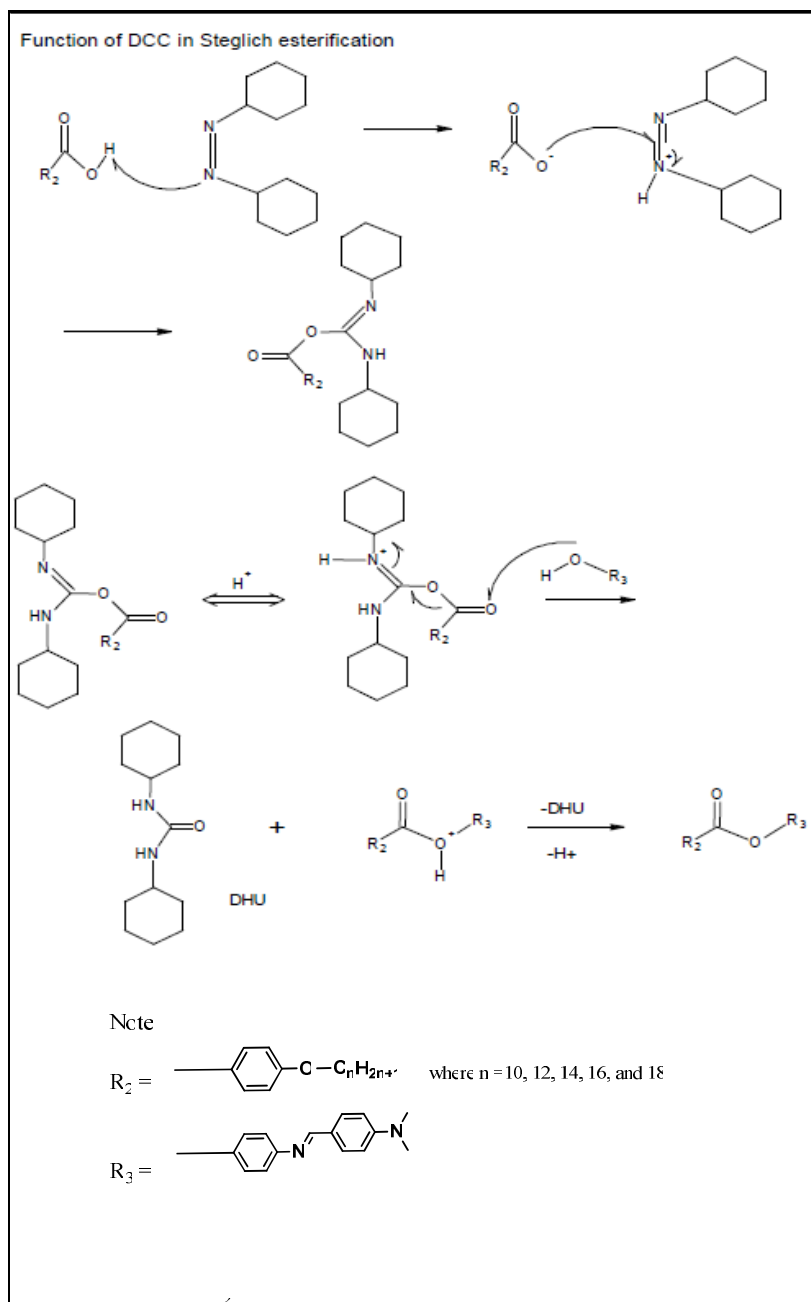


Figure 4.9: Mechanism of DCC with imine and carboxylic acid (Steglich Esterification)

Meanwhile, DMAP, as a nucleophile catalyst, the dimethylamino group acts as an electron donor substituent, increasing both nucleophilicity and basicity of the pyridine nitrogen (Carey and Sundberg, 2001), reacts with the O-acylisourea leading to a reactive amide ("active ester"). This intermediate cannot form intramolecular side products but reacts rapidly with alcohols. DMAP acts as an acyl transfer reagent in this way, and subsequent reaction with the alcohol gives the ester.

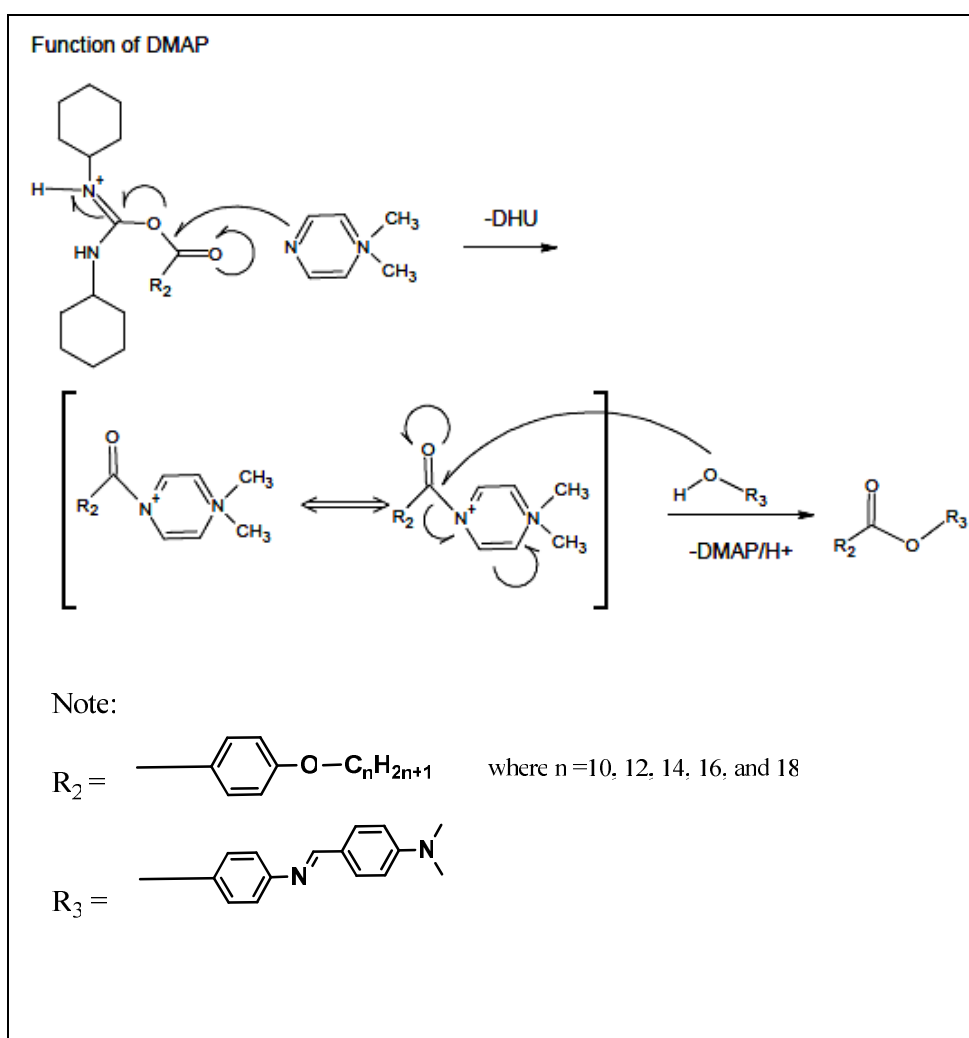


Figure 4.10: Function of DMAP

4.3 Mesomorphic Properties Analysis of nDMABAPB

4.3.1 Differential Scanning Calorimetry (DSC) Thermogram Analysis of nDMABAPB

DSC analyses have been carried out for all the compounds. The thermogram of the representative compound, **18DMABAPB** is shown in Figure 4.11.

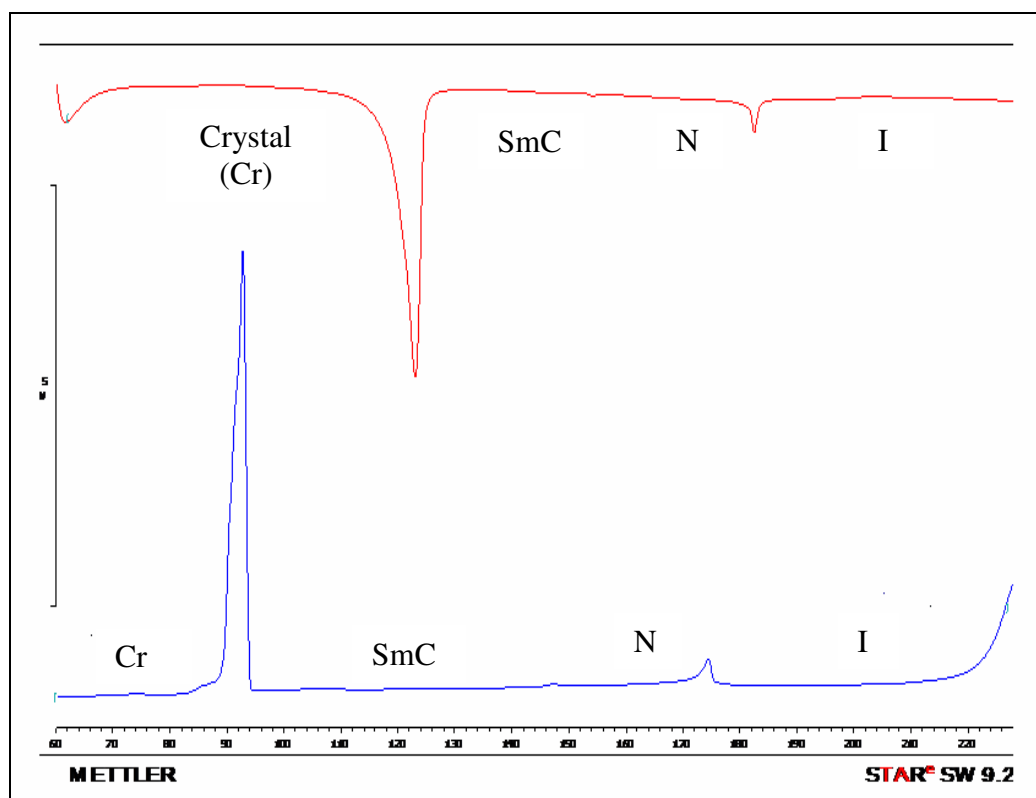
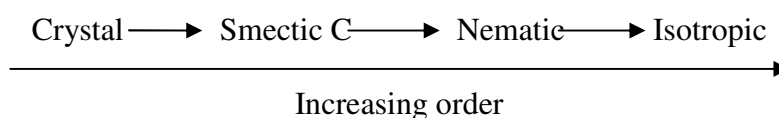


Figure 4.11: DSC thermogram of **18DMABAPB**

Upon heating, three peaks can be observed in the heating cycle at 122.99 °C (-38.37 kJmol⁻¹) where crystal is melted to a smectic C (SmC) phase liquid crystal. Further heating, to 154.03 °C (-0.12 kJmol⁻¹), nematic (N) liquid crystal was formed. When the heating is continued to 182.43 °C (-1.53 kJmol⁻¹), isotropic (I) liquid formed. All of the peaks indicated the endothermic energy absorbed the crystal molecules to break the intermolecular forces between molecules apart. It can be observed that the enthalpy change of SmC \longrightarrow N phase transition is smaller than the N \longrightarrow I phase transition. Meanwhile, the enthalpy changes for N \longrightarrow I phase transition are also smaller than Cr \longrightarrow SmC phase transition. This can be explained because due to liquid crystal are more similar to liquid, lesser latent heat is needed to convert liquid crystal to liquid compared to solid to liquid crystal.

There are three peaks which are observed in the cooling cycle. As the cooling cycle proceed, conversion of I \longrightarrow N occur at 174.43 °C (1.81 kJmol⁻¹), follows by phase transition of N \longrightarrow SmC at 147.15 °C (0.13 kJmol⁻¹). As the cooling process continues SmC \longrightarrow Cr take part at 92.9 °C (37.04 kJmol⁻¹). All these three peaks represent the exothermic energy was take place during the cooling cycle. This energy was released to reform the intermolecular bond. It is observed that phase transition of SmC \longrightarrow Cr has the highest enthalpy change as sufficient amount of energy is required to release in order to reform a complete crystalline arrangement with strong intermolecular forces. Phase transition between N and SmC only released small amount of energy as transition between

liquid crystal phases are very similar which is less ordered. The tendency of the series undergoes supercooling before recrystallization allows the smectic C phase to exhibit metastable state below the melting point. Thus, it is observed that smectic C occurs at larger temperature range compared to nematic phase. As the DSC analysis done for the **18DMABAPB**, the molecular orientation of the molecules is as below:



4.3.2 Influence of Alkanoyloxy chains on Transition Temperature Changes of nDMABAPB

The melting and clearing temperature of **nDMABAPB** are plotted as function of the number of carbons in the alkyl chain length in Figure 4.10 whereas the data are shown in Table 4.7.

Table 4.7: Transition temperatures of compounds **nDMABAPB**, where n = 10, 12, 14, 16 and 18, upon heating and cooling, obtained from DSC

Compound	Transition	Temperature (°C)	$ \Delta H $ (kJ mol ⁻¹)
10DMABAPB	Cr→N	128.53	26.25
	N→I	209.92	0.99
	I→N	203.31	1.31
	N→Cr	86.01	24.16
12DMABAPB	Cr→N	133.31	26.5
	N→I	189.27	0.45
	I→N	200.19	0.08
	N→Cr	80.58	21.31
14DMABAPB	Cr→N	134.15	38.21
	N→I	190.30	1.14
	I→N	183.86	1.17
	N→Cr	97.44	36.88
16DMABAPB	Cr→N	121.92	27.48
	N→I	180.86	1.19
	I→N	170.91	1.09
	N→Cr	79.68	28.45
18DMABAPB	Cr→SmC	122.99	38.37
	SmC→N	154.03	0.12
	N→I	182.43	1.53
	I→N	174.43	1.81
	N→SmC	147.15	0.13
	SmC→Cr	92.90	37.04

where Cr=Crystal; SmC=Smectic C; N=Nematic ; I=Isotropic

The region below the melting point shows crystalline phase region while above the clearing point belongs to isotropic liquid phase. Liquid crystal phase is observed between both melting and clearing in the graph (Figure 4.12).

It is observed that melting point is fluctuated as length of alkyl chain increases. However, the graph shows that it also have a trend line which shown the melting temperature is increases as the length of alkyl chain increases. This is due to the intermolecular forces which cause by the increase of length of alkyl chain. Meanwhile, the clearing point decreases as the length of alkyl chain increases. This happened mainly due to the dilution of the core group which induced by the increase in length of the alkyl chain.

As the melting point increases and the clearing point decreases when the alkyl chain become longer, it observed that the region of liquid crystal phase is become broader. As the alkyl chain getting longer, it will have tendency to balance the whole structure by the three rigid aromatic core where this increase the liquid crystal phase stability at higher alkyl chain. This can happened due to the flexibility of alkyl chain can be balanced by the three rigid aromatic core which cause the formation of liquid crystal to be more favourable at higher alkyl chain.

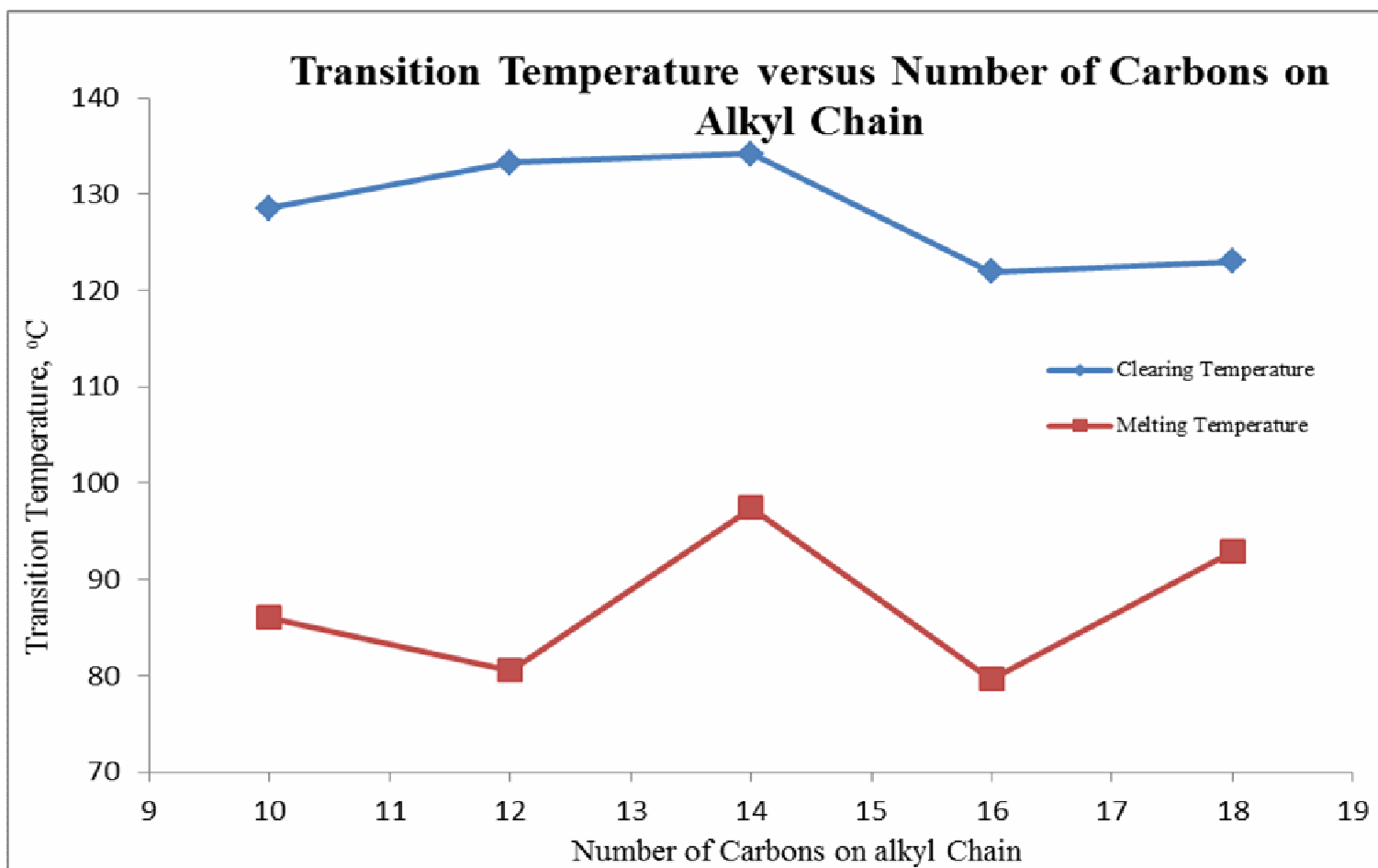
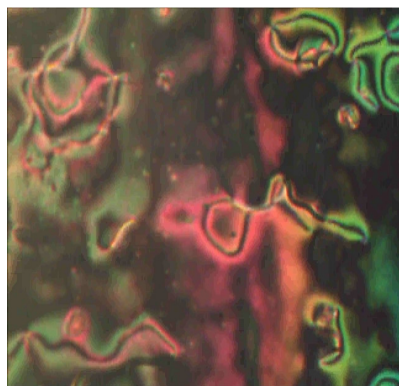


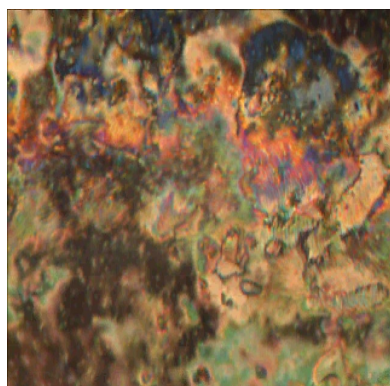
Figure 4.12: Graph of Transition Temperature versus Number of Carbons on Alkyl Chain

4.4 Polarising Optical Microscopy Studies of nDMABAPB

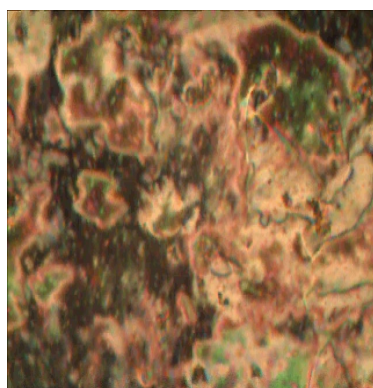
In this project, the mesomorphic behaviour of **nDMABAPB** series is studied under the polarising optical microscopy. Based on the results obtained, all the compounds are monotropic nematic except **18DMABAPB** which shown both smectogen and nematic properties. This series has shown the mesophase properties under heating and cooling process. Whole series which synthesized shown nematic phase where **18DMABAPB** shown both smectic C and nematic properties. The representative optical photomicrographs for **10DMABAPB** and **18DMABAPB** upon cooling cycle are shown in Figure 4.13.



(a)



(b)



(c)

Figure 4.13: Optical photomicrograph of **nDMABAPB** taken during cooling cycle. (a) Optical photomicrograph of compound **10DMABAPB** exhibiting thread-like textures of nematic phase (b) Optical photomicrograph of **18DMABAPB** exhibiting transition from nematic phase to (c) marble-like texture of SmC phase

From all the compound which have synthesized, **18DMABAPB** was the only compound that shown two liquid crystal phases which were smectic C and nematic phases. Hence, for **18DMABAPB**, it is cooling from isotropic to nematic and followed by smectic C phase and finally, crystal phase was all observed under POM. It can be deduced that smectic C phase exists n this mesogen because there are homeotropic texture and homogeneous filed (marble-like texture) coexisted for after the blinking droplets disappear. The marble-like texture of a smectic C phase was believed develops from the nematic phase as batonnets that coalesce and eventually generate the marble-like texture (Singh and Dunmur, 2002).

Meanwhile, **10DMABAPB** shown only nematic mesomorphic phase as when it cooled from isotropic to nematic phase and finally to crystal phase. From the observation under POM, **10DMABAPB** compound showed to posses a thread-like nematic texture. According to Collings and Hird, 1998, when the molecules are highly not aligned homeotropically, the phase structure adopts thread-like nematic texture. By compared the **10** and **18DMABAPB**, both of the compounds exhibit nematic structure. However, when the length of the alkyl terminal chain increases, the smectic tendency increase and eventually eliminates the nematic phase. This is because long terminal chains become intertwined, which facilitates the lamellar packing required for smectic phase generation (Collings *et al.*, 1998). Hence, for the entire compound, only **18DMABAPB** gives smectic C and nematic phase whereas the rest only exhibit nematic phase.

4.5 Structural Comparison with Related Compounds Reported in the Literature

Figure 4.14 shown the structures of **10DMABAPB** (current work) is used for the comparison with **10DBDMAA**, Han *et al.* (2006) and **CBDAAB** Neubert *et al.* (1995). The data are tabulated in Table 4.8.

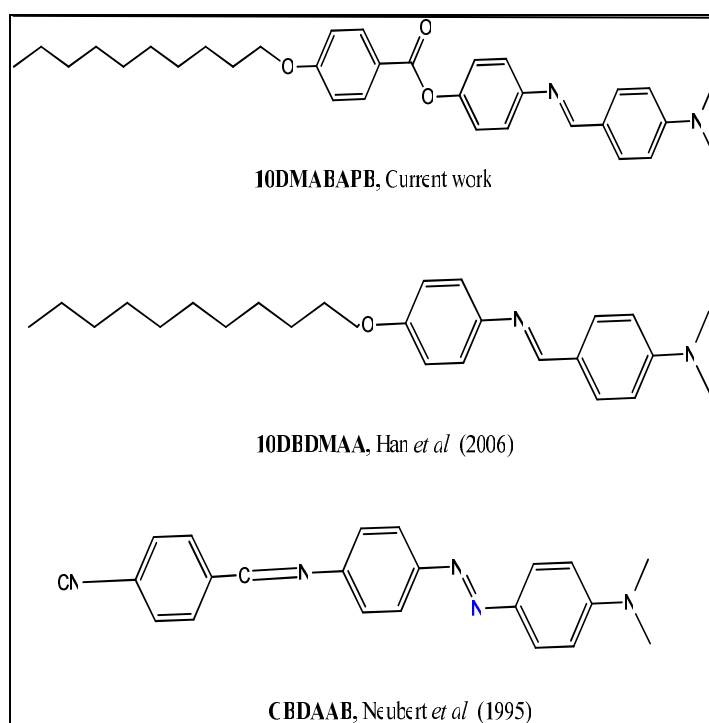


Figure 4.14: Structural Comparison with related compounds reported in the literature

Table 4.8: Transition temperature ($^{\circ}\text{C}$) for **10DMABAPB**, **10DBDMAA**, and **CBDAAB**

Compounds	Heating ($^{\circ}\text{C}$) / [Cooling ($^{\circ}\text{C}$)]	Mesophase range for cooling ($^{\circ}\text{C}$)
10DMABAPB	Cr 128.53 N 209.92 I / [Cr 86.01 N 203.31 I]	81.39 / 117.3
10DBDMAA	Cr 104.8 I / [Cr 88.5 N 94.9 I]	6.4
CBDAAB	[Cr 88.5 N 94.9 I]	31.8

In comparative between **10DMABAPB** and **10DBDMAA**, both shown monotropic nematic phase but however for **10DBDMAA**, it does not show the nematic phase during heating cycle. This is due to the presence of a carbonyl group where it's associated with an ester linkage plus an additional aromatic ring. Ester linkage is a planar linkage with a degree of polarizability due to the π electrons and associated with the carbonyl group plus an additional aromatic ring which adds the π electrons effect due to delocalised of an electron. This however cause the ester link confers a stepped structure but the linearity is maintained. The

stepped structure would tend to reduce the nematic phase stability because of the increased molecular breadth which tends to disrupt the lamellar packing.

For **10DMABAPB**, it has a wider nematic range compared to **CBDAAB**. This is due to the compound contains higher alkyl terminal side chain where it increased the liquid crystal phase stabilities compared to shorter C=N terminal group. The long alkyl chain reduces the lamellar packing and hence generates wider nematic range. Certain polar terminal group in such as cyano group confer a high birefringence. However, longer terminal alkyl chain exhibit higher birefringence than does a cyano group.

CHAPTER 5

CONCLUSION

A series of calamitic liquid crystal, 4-((4-(dimethylamino)benzylidene)amino)phenyl-4-(alkanoyloxy)benzoate, **nDMABAPB** (where n= 10, 12, 14, 16 and 18) was successfully synthesized.

The structure of all the liquid crystalline that have been synthesized has been elucidated by FT-IR, ¹H and ¹³C NMR spectroscopy and EI-MS. By analysed all the data obtained from the spectroscopic techniques, all the compounds were successfully synthesized. The final compounds are listed as below:

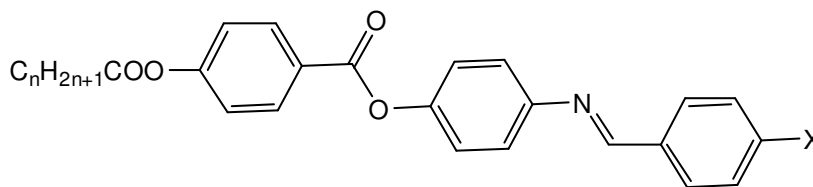
1. 4-((4-(dimethylamino)benzylidene)amino)phenyl-4-(decyloxy)benzoate,
10DMABAPB
2. 4-((4-(dimethylamino)benzylidene)amino)phenyl-4-(dodecyloxy)benzoate,
12DMABAPB
3. 4-((4-(dimethylamino)benzylidene)amino)phenyl-4-(tetradecyloxy)benzoate, **14DMABAPB**
4. 4-((4-(dimethylamino)benzylidene)amino)phenyl-4-(hexadecyloxy)benzoate, **16DMABAPB**

5. 4-((4-(dimethylamino)benzylidene)amino)phenyl-4-(octadecyloxy)benzoate,
18DMABAPB

The liquid crystal properties were studied by conducted several methods such as DSC and POM. Based from the DSC results, it reveals the presence of phase transitions in material by detecting the enthalpy change associated with each phase transition. Meanwhile, by observation under POM, all the final compounds that have been synthesized shown monotropic behaviour with thread-like texture of nematic phase. However, for the **18DMABAPB**, it exhibit both SmC and nematic phase.

Further Study

In further study, the lateral terminal dimethylamino group can be replaced with another polar group such as halogens, x. The polar group that conjugation with an aromatic core will confers a high birefringence.



where x = F, Cl, Br, I

References:

Journals:

Fornasieri, G., Guittard, F. & Géribaldi, S. (2003). Influence of the structure of the mesogenic core on the thermotropic properties of ω -unsaturated fluorinated liquid crystals. *Liquid Crystals*, 30(2), 251-257.

Galewaki, Z. (1994) Liquid crystalline properties of 4-halogenobenzylidene-4'-alkoxyanilines. *Mol. Cryst. Liq. Crystal.*, 249, 43-49.

Gray, G. W. (1983). *The Chemistry of Liquid Crystals*, Philosophical Transactions of the Royal Society of London, Series A, 309, 77-92.

Han Sang-Hee, Hirohisa Yoshida, Fumiyasu iwahori and Jiro Abe. (2006). Mesomorphic behaviors and photoconductive properties of binary systems composed of electron donor and acceptor mesogens. *Science and Technology of Advanced Materials*, 7(1), 62-7.

Neubert, M. E., Hummel, S. J., Bhatt, J. C., Keast, S. S., Lackner, A. M., Margerum, J.D. and Sherman, E. (1995). Synthesis and characterization of some azo-anil dyes. *Molecular Crystals and Liquid Crystals*, 260, 287 – 300.

Sie-Tiong Ha, Lay-Khoon Ong, Yasodha Sivasothy, Guan-Yeow Yeap, Hong-Cheu Lin, Siew-Ling Lee, Peng-Lim Boey and Nilesh L. Bonde (2010). Mesogenic Schiff base esters with terminal chloro group: Synthesis, thermotropic properties and X-ray diffraction studies. *International Journal of the Physical Sciences*, 5(5), 564-575.

Sie-Tiong Ha, Mei-Yoke Ng, Ramesh T. Subramaniam, Masato M. Ito, Ayumu Saito, Masaaki Watanabe, Siew-Ling Lee and Nilesh L. Bonde, (2010). Mesogenic azomethine esters with different end groups: Synthesis and thermotropic properties. *International Journal of the Physical Sciences*, 5(8), 1256-1262.

Timothy M. Swager, Paul H. J. Kouwer, (2007). Synthesis and Mesomorphic Properties of Rigid-Core Ionic Liquid Crystals. *J. Am. Chem. Soc.* 129, 14042-14052.

Wu, Y., Jiang, S. and Ozaki Y. (2004). Two-Dimensional Spectroscopy Study on Phase Transition and Structural Variations of a Hydrogen-Bonded Liquid Crystal. *Spect. Act.* 60, 1931-1939.

Yeap, G. Y., Ha, S. T., Lim, P. L., Boey, P. L., Ito, M. M., Sanehisa, S. and Vill, V. (2006). Nematic and smectic A phases in the ortho-hydroxy-para-hexadecyloxybenzylidene-para-substituted anilines. *Molecular Crystals and Liquid Crystals*, 452, 63 – 72.

Yeap, G. Y., Ha, S. T., Lim, P. L., Boey, P. L., Ito, M. M., Sanehisa, S. and Vill, V. (2006a). Nematic and Smectic a Phases in Ortho-Hydroxy-Para-Hexadecanoyloxbenzylidene-Para-Substituted Anilines. *Mol. Cryst. Liq. Cryst.*, 452, 63-72.

Book Chapter:

Collings, P.J. and Hird, M. (1998). *Introduction to liquid crystals chemistry and physics*. London: Taylor and Francis.

Dierking, I. (2003) *Texture of liquid crystals*, United Kingdom, Wiley-Vch Verlag.

Firch, R.M., (2006) *Liquid crystal, laptops and life*, USA, World Scientific.

Iam-Choon Khoo, (2007) *Liquid Crystals, Second Edition*, John Wiley & Sons, Inc., New Jersey, USA.

Pavia, D.L., Lampman, G.M. and Kriz, G.S. (2001), *Introduction to liquid Spectroscopy*, 3rd Edition (Pages 13-153). Washington Brooks and Cole.

Singh, S. and Dunmur, D.A. (2002). Liquid crystals: fundamentals. Danvers:
World Scientific Publishing Co. Pte. Ltd.

Website:

Dr. Mary Neubert (2010). Liquid Crystal phases, URL:

<http://plc.cwru.edu/tutorial/enhanced/files/lc/phase/phase.htm>. Accessed on
22 June 2010.

History of liquid crystals, (2010). URL:

http://www.lci.kent.edu/lc_history.html. Accessed on 25 June 2010.

History and Properties of Liquid Crystals , (2010). Nobelprize.org. URL:

http://nobelprize.org/educational/physics/liquid_crystals/history/. Accessed
on 25 June 2010.

Liquid Crystals, (2010). Wikipedia, the free encyclopaedia, Wikipedia, URL:

http://en.wikipedia.org/wiki/Liquid_crystal. Accessed on 22 June 2010.

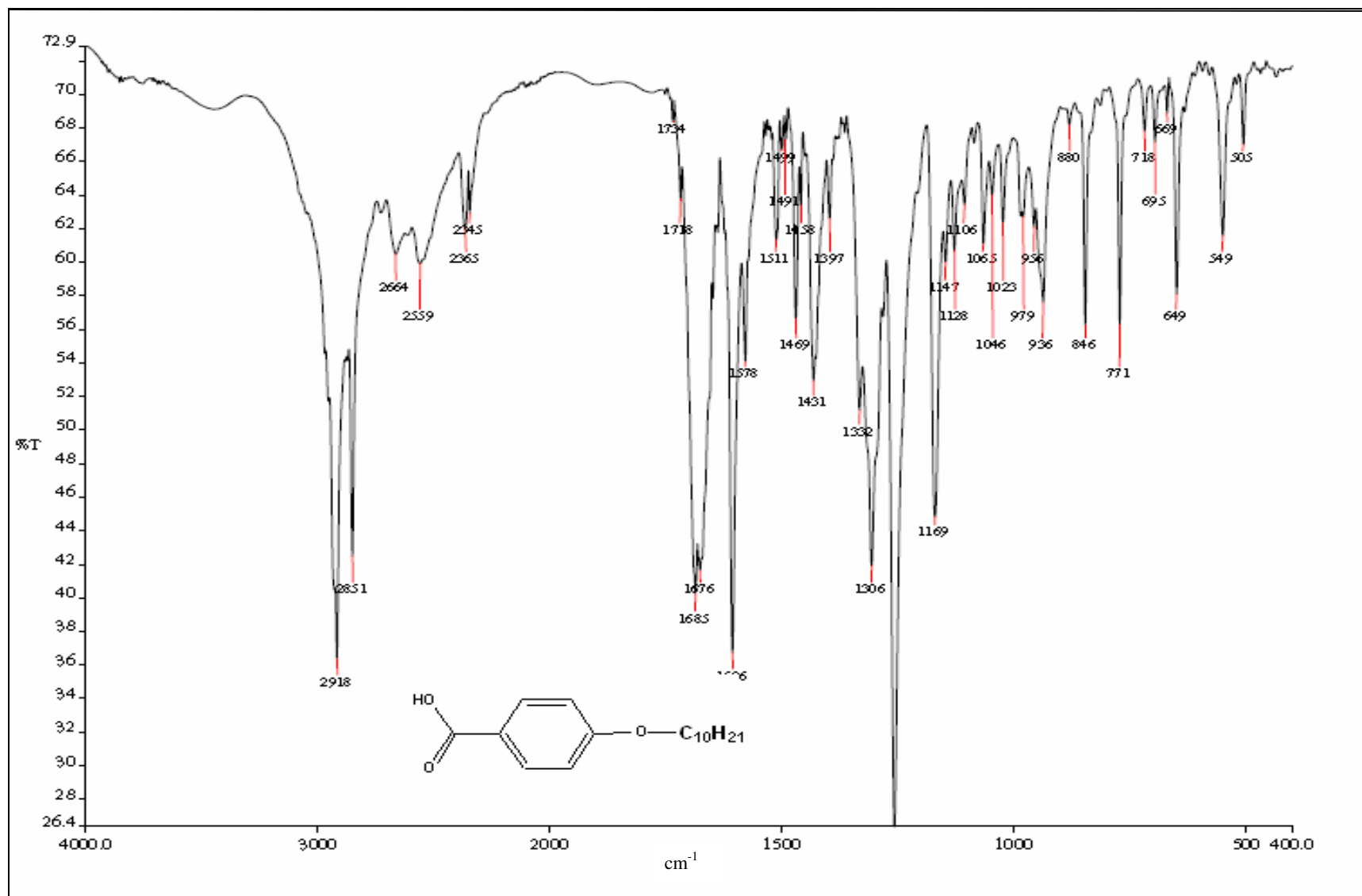
Steglich Esterification, URL:

[http://www.organic-chemistry.org/namedreactions/steglich-
esterification.sthm](http://www.organic-chemistry.org/namedreactions/steglich-esterification.sthm). Accessed on 03th January 2011.

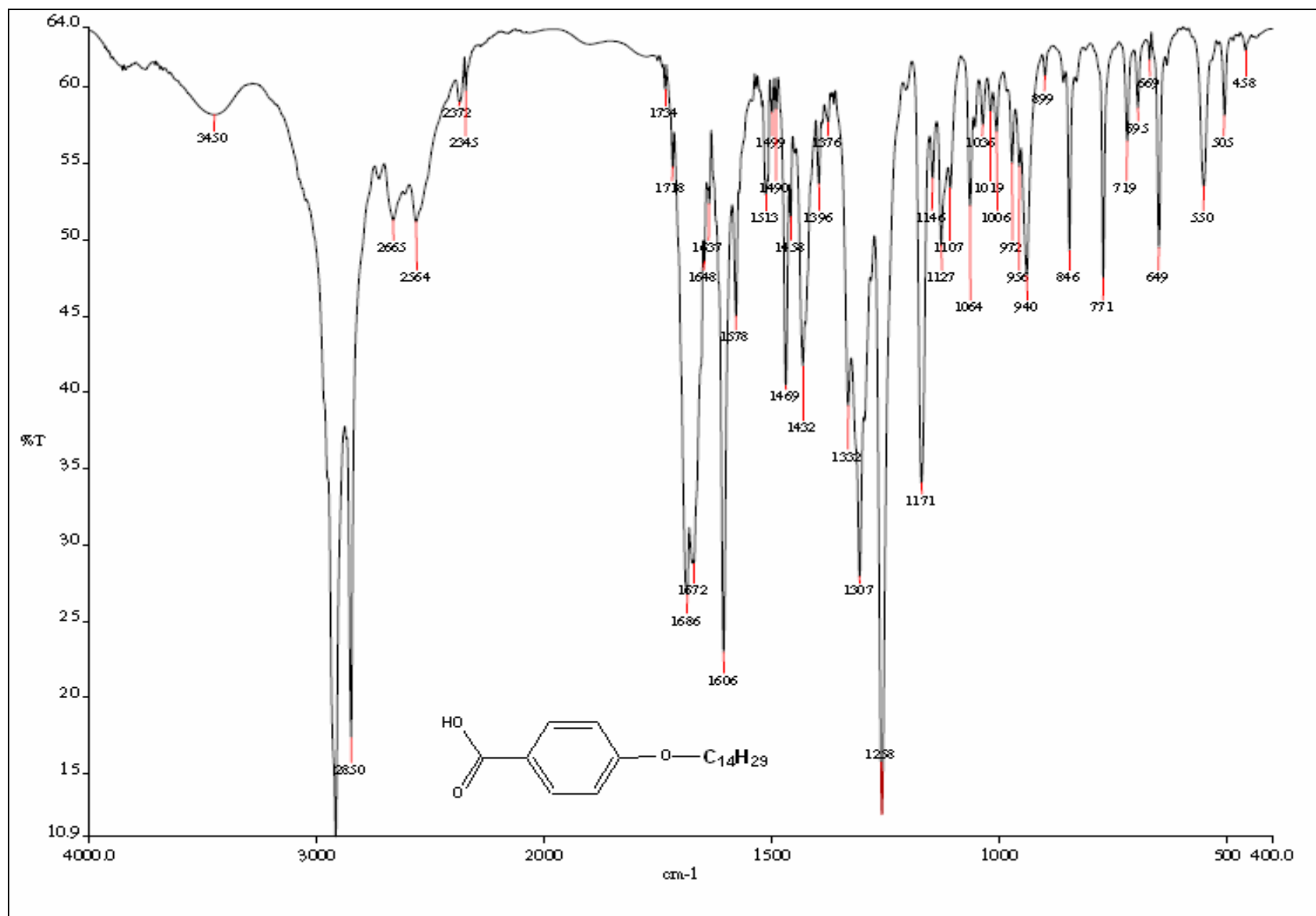
Imine Formation, URL:

<http://chemistry2.csudh.edu/rpendarvis/imineformF99.html>.

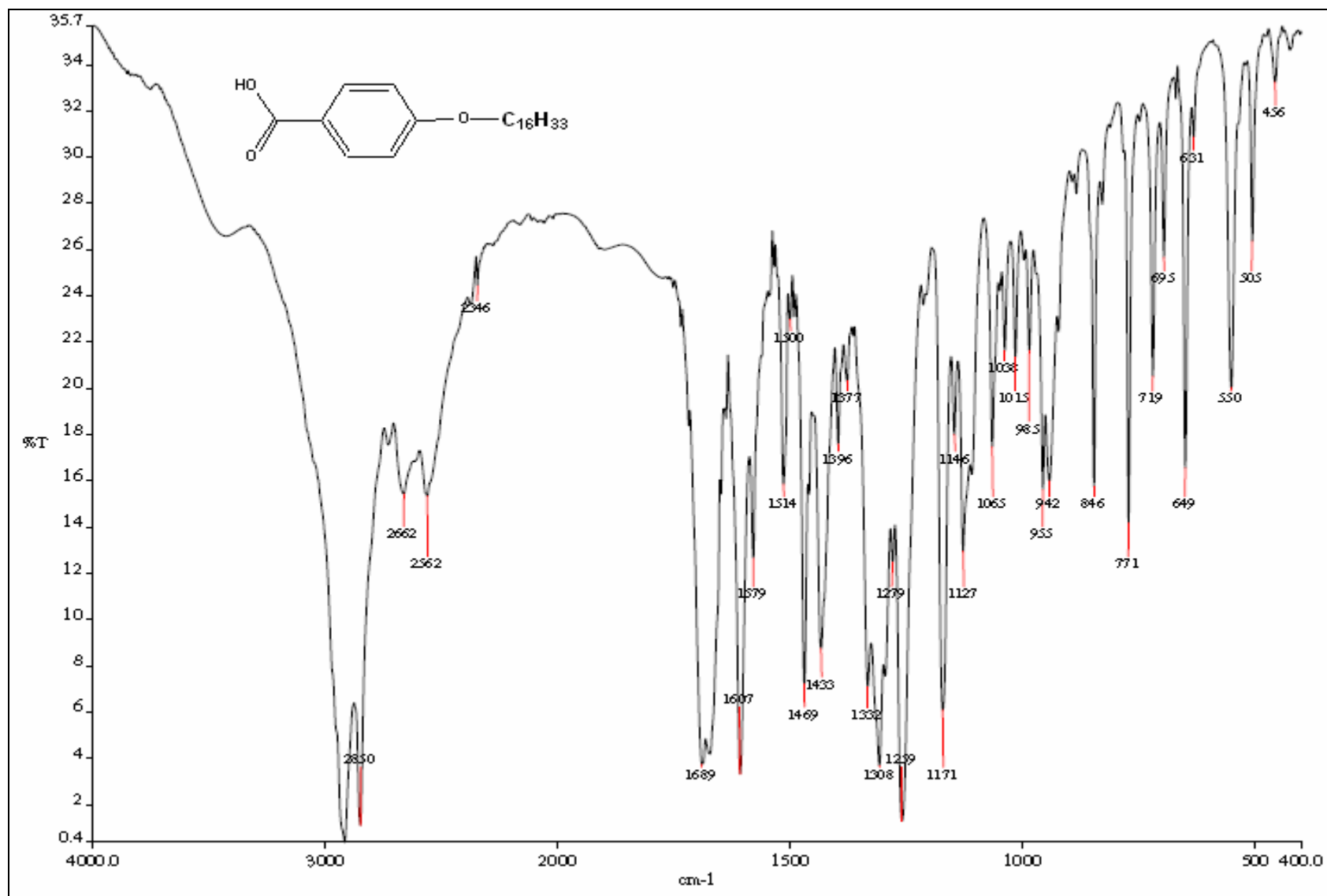
Accessed on 03th January 2011.



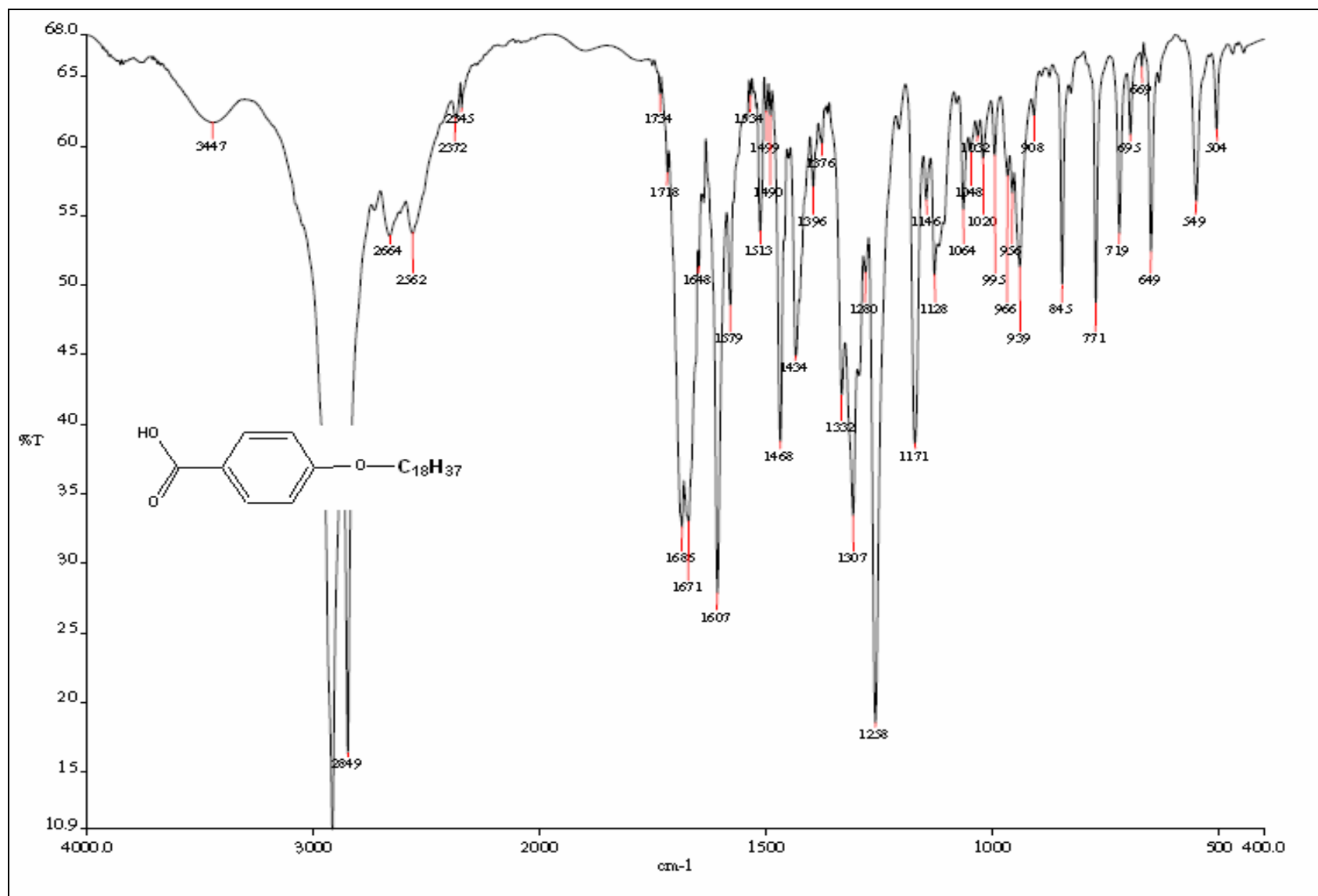
A1 FTIR Spectrum of 10ABA



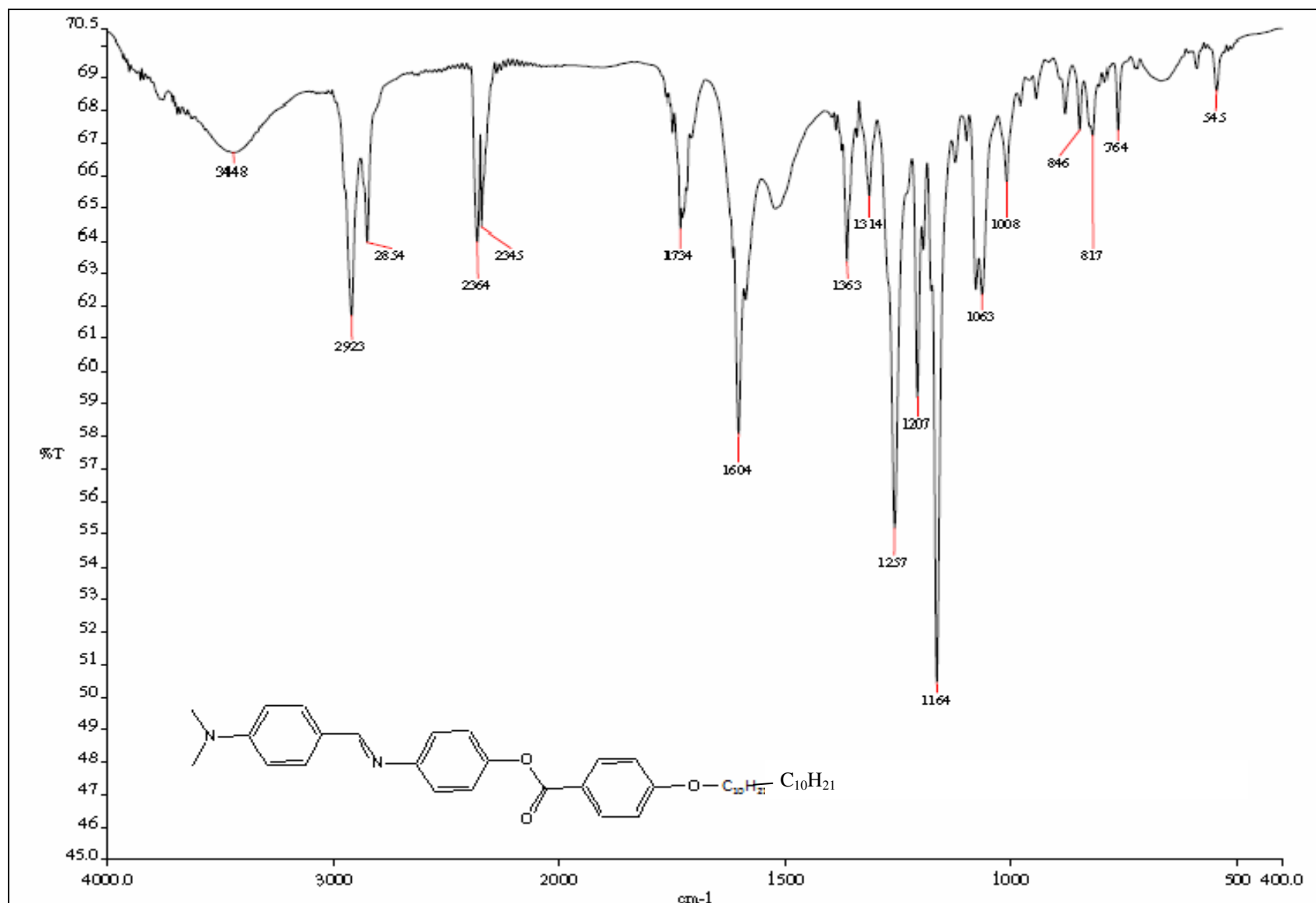
A2 FTIR Spectrum of 14ABA



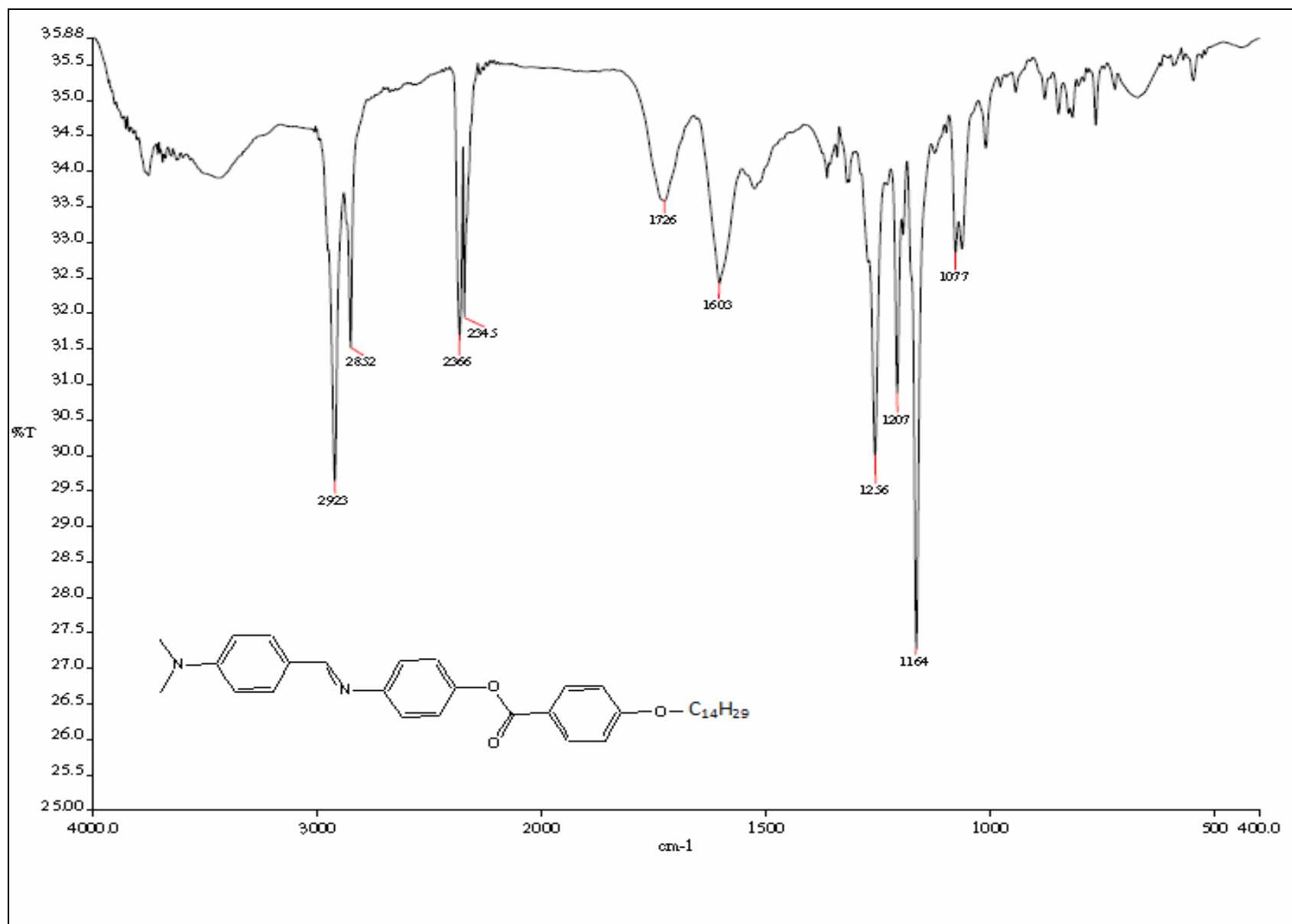
A3 FTIR Spectrum of 16ABA



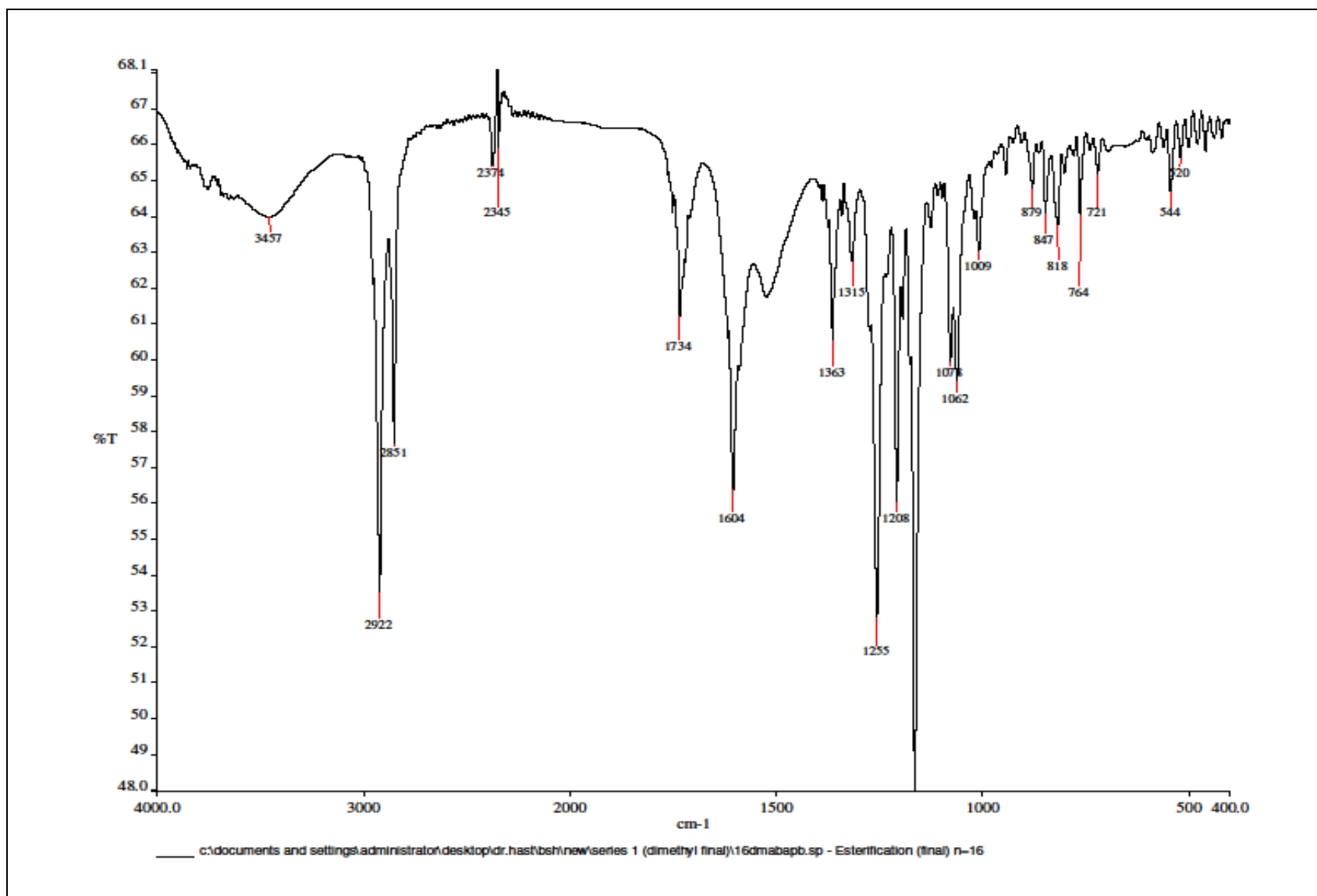
A4 FTIR Spectrum of 18ABA



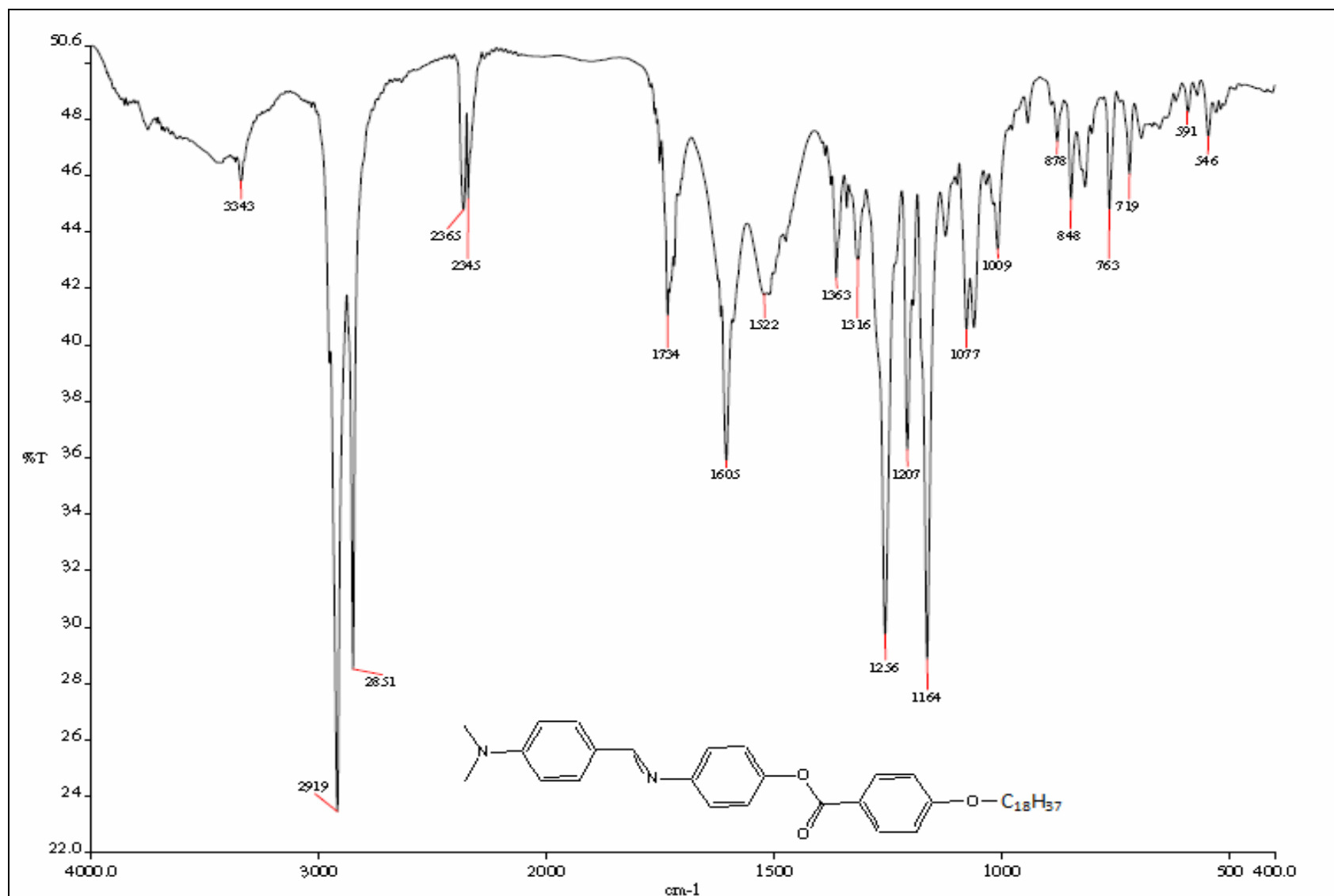
A5 FTIR Spectrum of 10DMABAPB



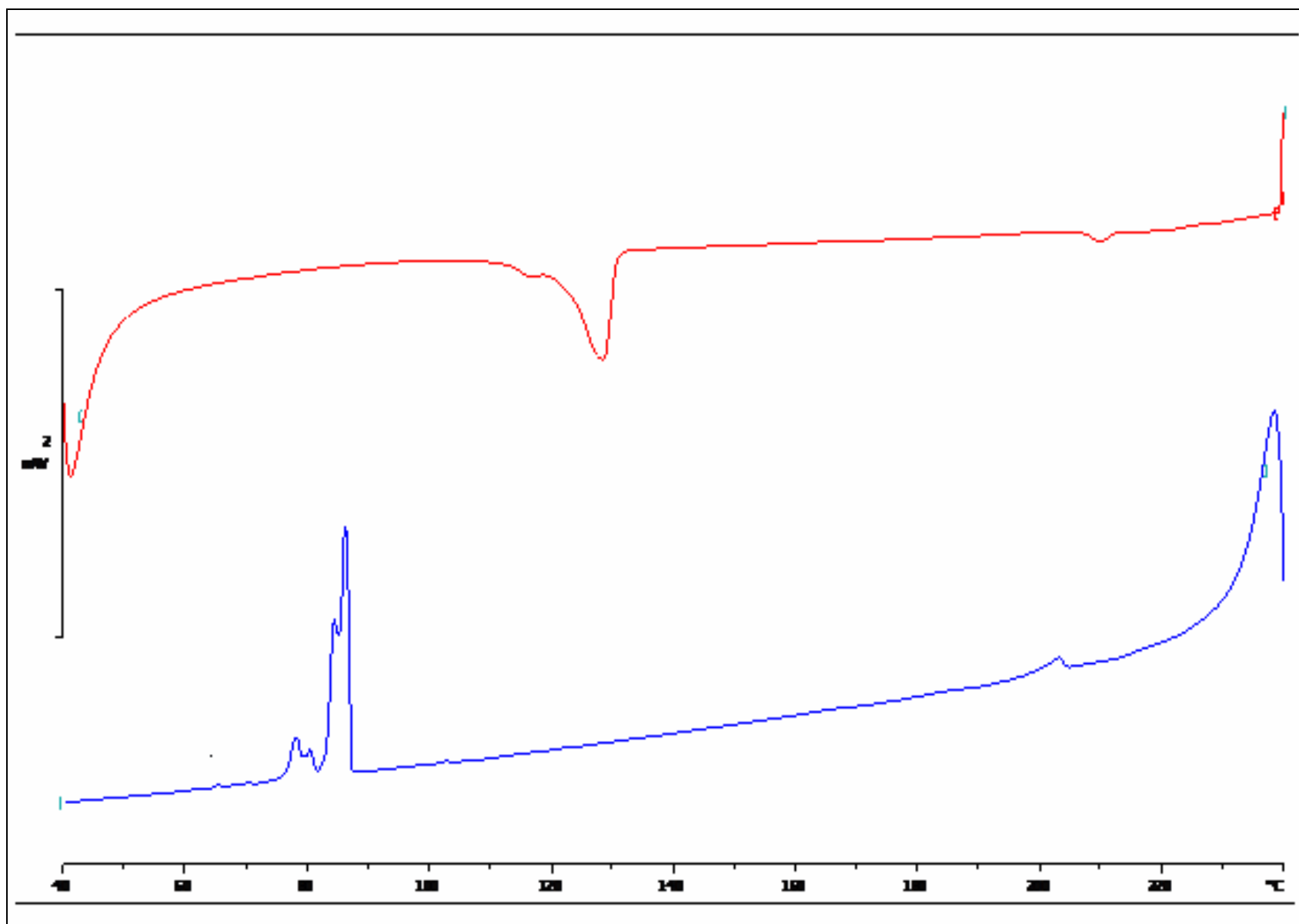
A6 FTIR Spectrum of 14DMABAPB



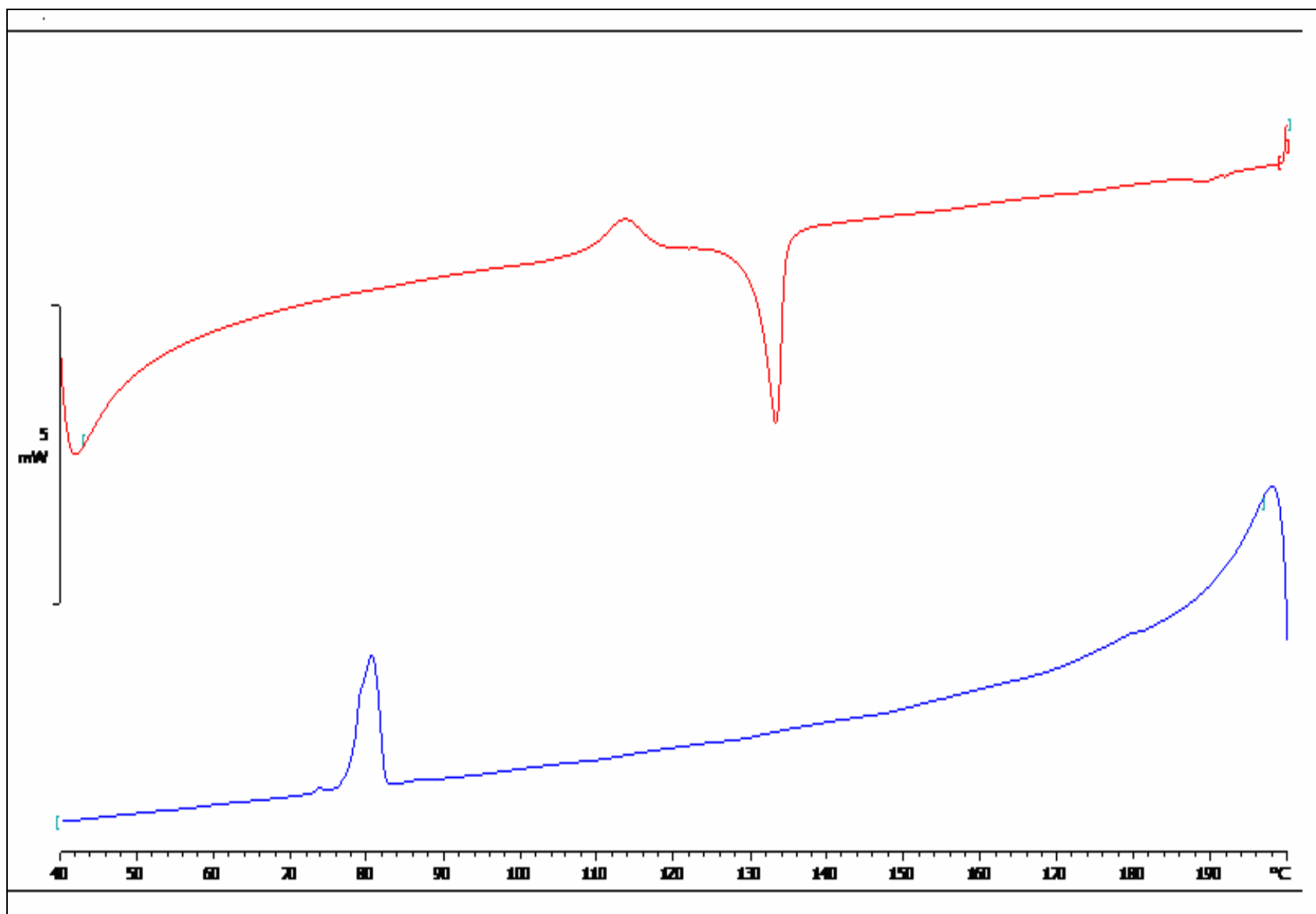
A7 FTIR Spectrum of 16DMABAPB



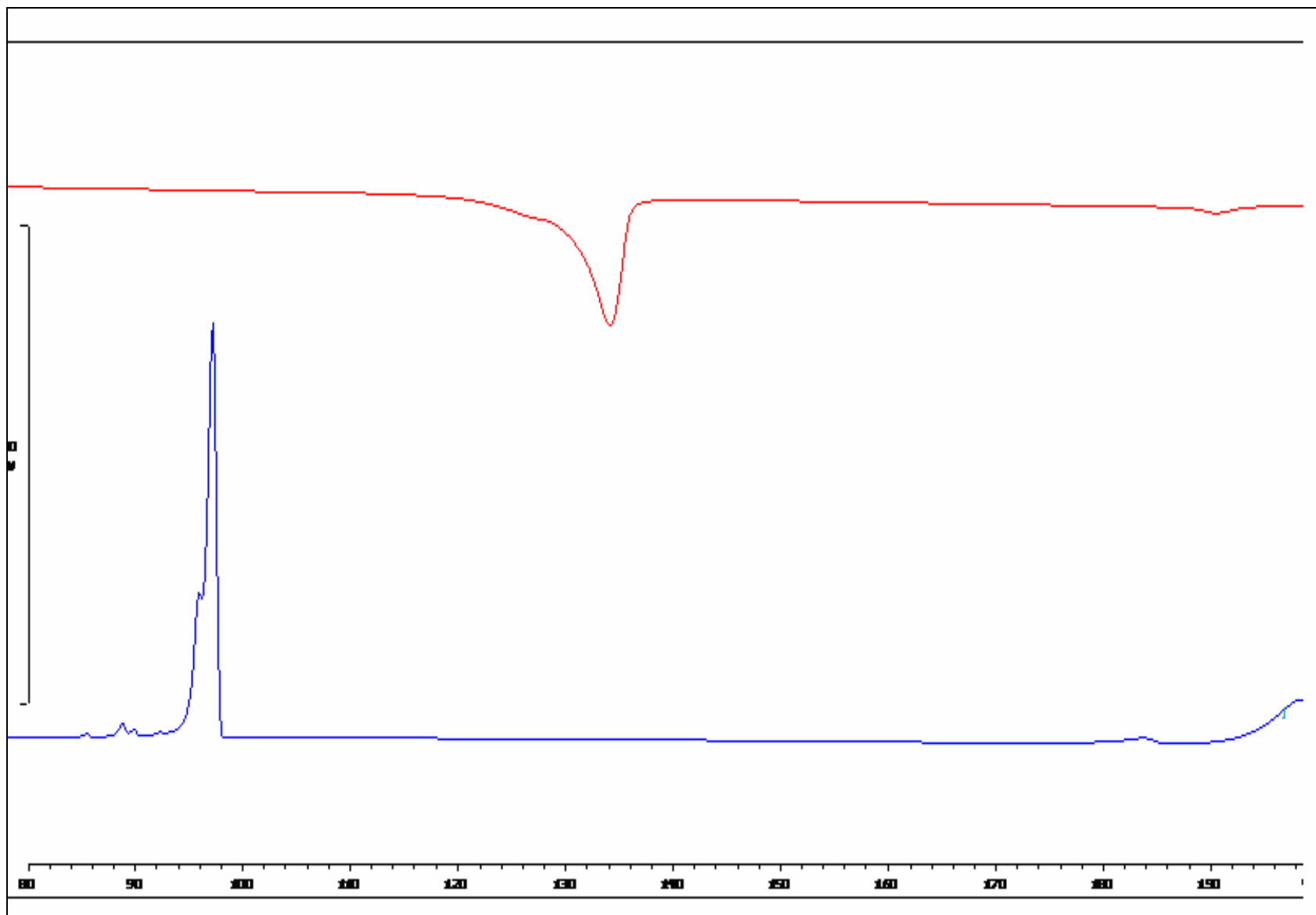
A8 FTIR Spectrum of 18DMABAPB



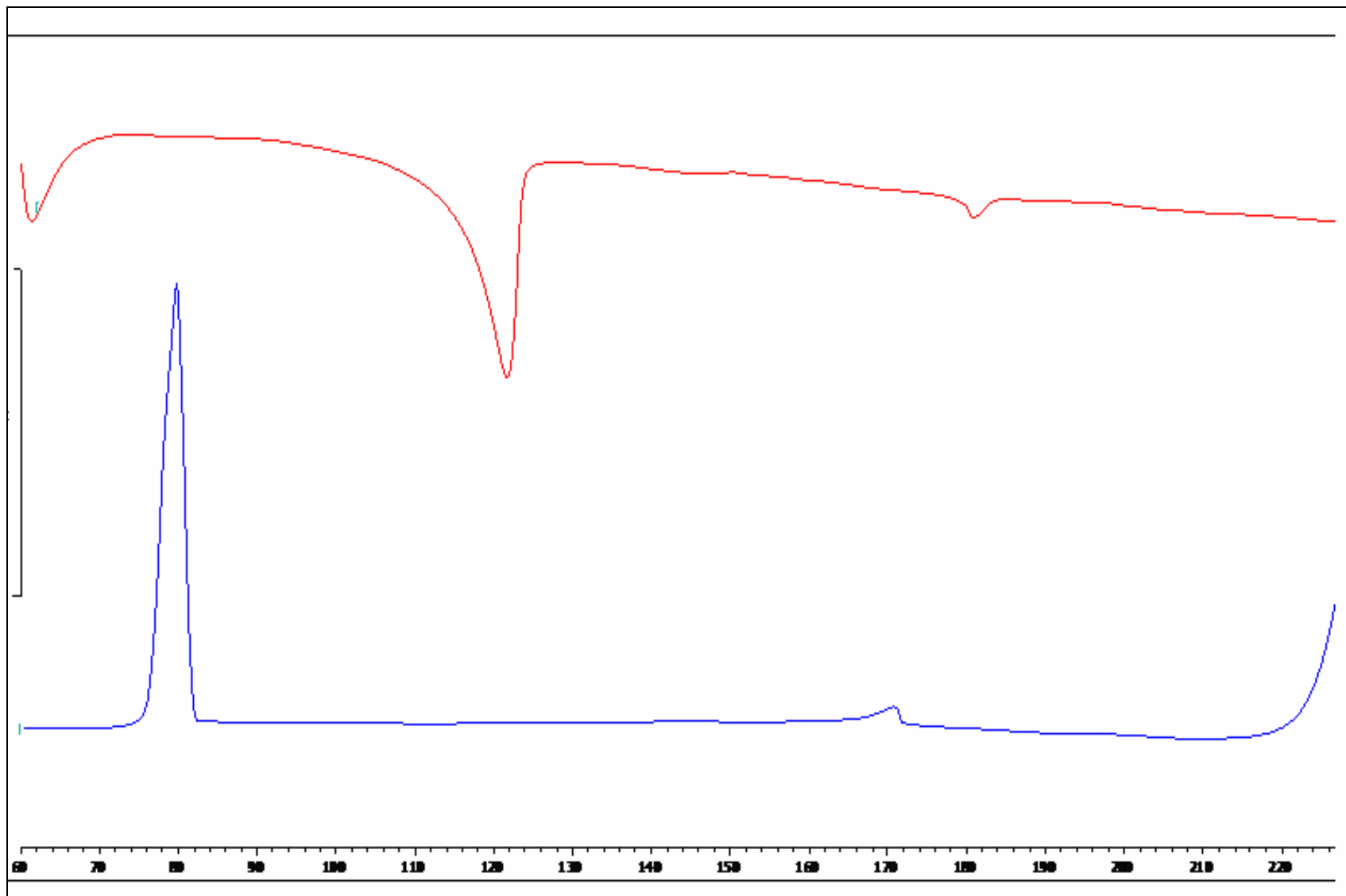
B1 DSC Thermogram for 10MABAPB



B2 DSC Thermogram for 12MABAPB



B3 DSC Thermogram for 14MABAPB



B4 DSC Thermogram for 16MABAPB